Environmental Factors and Pollution Stresses Select Bacterial Populations in Association With Protists

Songbao Zou, Qianqian Zhang, Xiaoli Zhang, Christine Dupuy, Jun Gong

Environmental Factors and Pollution Stresses Select Bacterial Populations in Association With Protists

Songbao Zou[1,2,3], Qianqian Zhang[1], Xiaoli Zhang[1], Christine Dupuy[4] and Jun Gong[3,5]*

[1] Yantai Institute of Coastal Zone Research, Chinese Academy of Sciences, Yantai, China, [2] University of Chinese Academy of Sciences, Beijing, China, [3] School of Marine Sciences, Sun Yat-sen University, Zhuhai, China, [4] Littoral Environnement et Sociétés (LIENSs) UMR 7266 CNRS, University of La Rochelle, La Rochelle, France, [5] Southern Marine Science and Engineering Guangdong Laboratory (Zhuhai), Zhuhai, China

Digestion-resistant bacteria (DRB) refer to the ecological bacterial group that can be ingested, but not digested by protistan grazers, thus forming a specific type of bacteria-protist association. To test the hypothesis that the environment affects the assembly of DRB in protists, a mixotrophic ciliate, *Paramecium bursaria*, and a heterotrophic ciliate, *Euplotes vannus*, were reared at different temperatures, light conditions, and concentration gradients of antibiotic oxytetracycline and heavy metals. Community profiling indicated that the composition of DRB in both species varied significantly across the manipulated conditions, except for in *P. bursaria* under light/dark treatments. Clone library analysis of bacterial 16S rRNA genes showed that DRB were diverse. *Pseudomonas* became more abundant during the warmer treatment of *P. bursaria*, whereas the dominance of *Pseudoalteromonas* weakened and *Vibrio* became more abundant in *E. vannus* at a higher temperature. During the treatment of diel light:dark cycles, *Aestuariibacter* and *Alteromonas* were selected for in *E. vannus* but not *Pseudoalteromonas*, which was highly represented in the all-light and all-dark treatments. In contrast, *P. bursaria* consistently hosted *Nevskia*, *Curvibacter*, and *Asticcacaulis* under all light conditions. There were many bacterial species co-resistant to oxytetracycline and to protistan digestion, in which *Sphingomonas, Alteromonas*, *Aestuariibacter*, *Puniceicoccaceae* (Verrucomicrobia), *Pseudomonas*, and *Sulfitobacter* were frequently abundant. *Flectobacillus* and *Aestuariibacter* were major lead-resistant bacteria associated with the studied protists. *Acinetobacter* and *Hydrogenophaga* were abundant in the *P. bursaria* treated with a high dose of mercury. *Aestuariibacter* was found as a dominant group of DRB in *E. vannus* across all cadmium treatments. In summary, this study demonstrates for the first time that environmental stress selects for bacterial populations associated with protists and that there are diverse bacterial species that not only are resistant to pollution stresses but can also survive protistan predation. This work highlights that bacteria-protists associations need to be taken into account in understanding ecological and environmental issues, such as resilience of bacterial community and function, microbial co-occurrence, and quantity and distribution of antibiotic resistant bacteria and genes.

Keywords: antibiotic resistance, interkingdom interaction, light, metal resistance, protozoa, warming

INTRODUCTION

Bacteria and protists are major players in the microbial food web of aquatic environments, in which heterotrophic bacteria incorporate dissolved organic matter and nutrients for growth and transfer carbon and energy to higher trophic levels as a consequence of predation by small protists (Azam et al., 1983). In the last two decades, much efforts have been made to understand how and why protists selectively graze on bacteria or how bacteria become resistant to protistan predation. It has been demonstrated that changes in bacterial cell size, morphology, movement, cell-cell configuration in space, and chemical resistance contribute to their anti-predation (Matz and Kjelleberg, 2005; Pernthaler, 2005; Jousset, 2012). Furthermore, recent studies have provided evidence for another strategy of anti-predation—some bacterial populations in aquatic environments can be ingested, but not digested by protistan grazers, thus potentially forming microbial associations with the protistan hosts (e.g., First et al., 2012; Šimek et al., 2013; Gong et al., 2014). When protistan isolates and assemblages are exposed in natural bacterial communities, the detected digestion-resistant bacteria (DRB) can be prevalent and diverse, showing a common trait in taxonomic composition where Gammaproteobacteria and Alphaproteobacteria usually dominate in marine samples (Martinez-Garcia et al., 2012; Pucciarelli et al., 2015; Farnelid et al., 2016; Gong et al., 2016). From an ecological point of view, the existence of DRB could prevent organic matter and energy from being transferred to protistan grazers and higher trophic levels via the microbial loop, adding another layer of complexity in the structure and functions of microbial webs.

Despite the ecological importance of DRB, associations between DRB and protists remain poorly understood. One issue is how environment and host affect the diversity and assemblage composition of the DRB associated with protistan populations. There are indications that pre-culture conditions would affect the ingestion and digestion of heterotrophic nanoflagellates (Boenigk et al., 2001). In our previous studies of DRB in ciliated protists cultivated in the laboratory or isolated directly from natural environments, we also observed that the DRB assemblage could substantially differ among host species and even for populations of the same species isolated at separate time points at an identical location, suggesting that the DRB diversity and assemblage composition can be both host- and environment-dependent (Gong et al., 2014, 2016). These relationships seem straightforward, since numerous studies have demonstrated that changes in physical and chemical factors drive bacterial abundance and community composition in bulk environmental samples via bottom-up controls or due to effects of pollutants (e.g., Storesund et al., 2015; Ibekwe et al., 2016).

It is well known that environmental factors play important roles in shaping the diversity and dynamic of the bacteria in a natural aquatic environment (Alonso-Sáez et al., 2006; Adams et al., 2010; Darriba et al., 2012; Hu et al., 2014). When the diversity of source bacteria shifts via environmental filtering, it is likely that different sets of bacterial populations are ingested by the protists and retained inside the cells for at least a short-term period, resulting in different assemblage structures of DRB accordingly. However, when the ingested bacteria escape from lysosomes, they enter into the cytoplasm of host cells, a relatively stable physical and chemical environment (due to cellular homeostasis), which may select for a specific group of DRB. However, it remains to be investigated if and how DRB assemblage associated with bacterivorous protists varies with environmental changes and under chemical stresses.

In this study, we performed microcosm experiments using two bacterivorous protist species, *Euplotes vannus*, a marine heterotrophic ciliate, and *Paramecium bursaria*, a freshwater ciliate with endosymbiotic green algae (*Chlorella* sp.). We aimed to test the following hypotheses: (1) warming, light condition, antibiotic, and heavy metal treatments would individually lead to significant changes in DRB assemblages of both ciliate species; (2) the changes in DRB assemblages in both ciliates were greater than the free-living bacterioplankton in the media; and (3) there were diverse bacteria co-resistant to antibiotics/metals and protistan digestion. We believe that the exploration of the diversity and variation pattern of DRB will improve our understanding of bacteria-protist interactions and the dynamics of microbial food webs.

MATERIALS AND METHODS

Source Organisms and Cultivation

The freshwater ciliate species *P. bursaria*, collected from a pond on the campus of Yantai University (Yantai, Shandong, China) in 2014, and the marine species *E. vannus*, isolated from the estuarine water of the Guangdang River (Yantai, China) in 2013, were investigated. The water used for cultivation was collected on site and treated by passing through a GF/C glass fiber filter (1822-047 grade, pore size: 1.2 µm, Whatman, United Kingdom), such that most pico-, nano-, and larger-sized organisms were removed, and the raw bacterioplankton was largely retained as food for the testing protists. The ciliate cells were observed under a stereoscope (XLT-400, Guilin Guiguang, Guangxi, China), individually selected with a micropipette, and washed for at least 3 times in sterile water to remove other protists and attaching bacteria. A few (3 to 5) cleaned cells were then inoculated into filtered water, allowing the stock cultures to develop. The stock cultures (each in 15 mL volume) were maintained in glass Petri dishes at 16°C for 2 weeks, with several rice grains to enrich bacterial prey (**Supplementary Figure S1**).

Experimental Settings

Different temperatures, illuminations, and stresses of antibiotics and heavy metals were set up to investigate the effects of environmental factors and pollution stresses on the diversity of DRB. For each treatment, about 30 ciliate individuals were picked up from the stock cultures and transferred into a Petri dish containing 20 ml aliquote of the filtered water, in which we assumed there was a bacterial community initially identical in quantity and community composition but subsequently being selectively grazed under various treatment conditions (**Supplementary Figure S1**). Effects of each factor were investigated independently, and each treatment was performed in

triplicate. To investigate the effect of temperature, the Petri dishes with stock ciliate cultures were incubated in three chemostats, which were set at a temperature of 16°C, 21°C, and 25°C, with other factors kept constant (e.g., with 12 h:12 h alternation of light and dark and good gas exchange). The experiments testing the effects of light and pollutant stresses were performed at a constant temperature of 25°C. Light treatments were maintained in consistently illuminated (LL), completely dark (DD), and 12 h:12 h alternation of light and dark conditions (LD).

The effects of pollution stresses on the DRB assemblage were carried out along gradients of the pollutants. To examine the effects of antibiotics, oxytetracycline, one of the most widely used antibiotics in farming industrials, was used in this study. The stock solution (100 mg/L) of oxytetracycline (OTC, Sigma, St. Louis, MO, United States) was added, drop-by-drop, to the ciliate cultures and gently mixed, resulting in final concentrations of 1, 10, and 20 mg/L (hereafter referred to as OTC1, OTC10, and OTC20, respectively). Three types of heavy metals, lead chloride ($PbCl_2$), cadmium chloride ($CdCl_2$), and mercury chloride ($HgCl_2$; AR grade; Sinopharm, Shanghai, China) were used at final concentrations as follows: 10, 30, and 50 mg/L for $PbCl_2$ (hereafter referred to as Pb10, Pb30, and Pb50); 0.01, 0.05, and 0.1 mg/L for $HgCl_2$ (hereafter referred to as Hg0.01, Hg0.05, and Hg0.1); and 0.1, 0.5, and 1 mg/L for $CdCl_2$ (hereafter referred to as Cd0.1, Cd0.5, and Cd1). Since neither *P. bursaria* in the Cd treatments nor *E. vannus* in the Hg treatments survived, these treatments were not included in the subsequent analyses. The cultures without any amendments of antibiotic and heavy metals (i.e., the treatments OTC0, Pb0, Hg0, and Cd0) were taken as the controls.

For molecular assays of DRB inside the protistan cells, approximately 20-30 ciliate cells in all of these treatments were isolated during their exponential growth stages, which usually took place within 8 days of cultivation according to our pilot studies. In order to minimize the contamination from the bacteria attached to the cell surface and the cilia, protistan cells from these treatments were washed repeatedly (at least three times) by transferring to a series of sterilized seawater (for *E. vannus*) or autoclaved Milli-Q water (for *P. bursaria*) with a clean micropipette. These cleaned ciliates were then maintained in the sterilized water for two or three days, allowing the ingested bacteria to be digested as much as possible. The remaining bacteria inside these ciliate cells were considered DRB. Since the free-living bacteria in the culture medium were apparently sources for the DRB, the diversity of the former might be altered under different conditions, which was a potential mechanism modulating the diversity of the latter. To investigate this, therefore the ciliate-free culture medium was also collected for analyzing the free-living bacterial community composition and structure in each treatment.

DNA Extraction, Clone Libraries, and Sequencing

Three to five ciliate individuals with a minimum volume of water were transferred to a microfuge tube for DNA extraction using a REDExtract-N-Amp Tissue PCR Kit (Sigma, St. Louis,

MO, United States), according to the modified protocol (Gong et al., 2014). Furthermore, the DNA of bacterioplankton was prepared by taking 3 µL of ciliate-free culture medium from each treatment using the same method.

The identities of the DRB were revealed using PCR amplification, clone library construction, and sequencing of bacterial 16S rRNA genes. PCR was carried out in a Applied Biosystems Veriti® 96-Well thermal cycler (Foster City, CA, United States), with universal bacterial 16S rRNA gene primers 27F1 (5′-AGAGTTTGATCCTGGCTCAG-3′) and 1492R (5′-GGTTACCTTGTTACGACTT-3′) (Lane, 1991), or 63F (5′-CAGGCCTAACACATGCAAGTC-3′) and 1389R (5′-ACGGGCGGTGTGTACAAG-3′) (Osborn et al., 2000). Each PCR reaction cocktail contained 1 µL of 10 µM forward and reverse primers, 1 µL of template DNA, 2.5 µL of 10 × PCR buffer, 2.5 µL of 25 mmol/µL $MgCl_2$, 0.5 µL of 10 mmol/µL dNTP, and 0.2 µL of 1 U *Taq* DNA polymerase (Fermentas, Thermo Scientific, Waltham, MA, United States), and deionized water was added to a final volume of 25 µL. The PCR reactions were programmed as follows: an initial denaturation step at 94°C for 3 min, followed by 35 cycles of 30 s denaturation at 94°C, 1 min annealing (primers 27F/1492R at 50°C, and primers 63F/1389R at 52°C), and a 2 min elongation at 72°C, with a final extension step of 72°C for 7 min. Subsequently, all PCR products were visualized on 1% agarose gels, which contained GoldView (Solarbio, Beijing, China). The target bands were excised, purified by a TIANquick Midi Purification Kit (Tiangen, Beijing, China), inserted into PTZ57 R/T vectors using the InsTAclone PCR Clone Kit (Fermentas), and transferred to the competent cells Trans5α (TransGen Biotech, Beijing, China) in order to construct the clone libraries. A total of 108 clone libraries were constructed, with about 50 positive clones randomly selected for pre-screening, which was conducted using restriction fragment length polymorphism (RFLP) analysis with *Taq* and *Hha*I, two FastDigest restriction enzymes (Thermo Scientific, Waltham, MA, United States). About 20–30 clones in each library were sequenced on an automated ABI 373 DNA sequencer (Applied Biosystems) in a commercial sequencing service company (Sangon Biotech, Shanghai, China).

The 16S rRNA gene sequences (about 1300 bp in length) obtained from cloning and sequencing were aligned using MAFFT v.7.0 with default parameters (Katoh and Standley, 2013). Potential chimeras were identified using Bellerophon (Huber et al., 2004) and Mallard 1.02 (Ashelford et al., 2006) and discarded before subsequent analysis. The cleaned sequences were clustered into operational taxonomic units (OTUs) at 97% identity using Mothur v.1.17 (Schloss et al., 2009). Taxonomic identities and systematic placements of the OTUs were assigned using the RDP Classifier (release 11.5) (Wang et al., 2007). The 16S rRNA gene sequences have been deposited in the GenBank databases with accession numbers MH555909 to MH556816.

Phylogenetic Analyses

For several sequences that assigned into unclassified Bacteroidetes and Verrucomicrobia by the RDP classifier, phylogenetic analyses were carried out using both maximum

likelihood (ML) and Bayesian inference (BI) algorithms to further resolve their taxonomic ranks. Reference sequences of previously described species were retrieved from the GenBank database and aligned with the sequences in question using MAFFT. The alignment was refined manually using SeaView4 (Galtier et al., 1996). The models of nucleotide substitution were estimated using jModeltest2 (Darriba et al., 2012) based on Akaike information criterion (AIC) and Bayesian information criterion (BIC). The ML analysis was conducted using PhyML v.3.3 (Guindon et al., 2009) with a best-fit GTR + I + G evolutionary model and 1000 bootstrap replicates. The BI trees were generated using MrBayes 3.2.7 with selected parameters (rates = invgamma, number of substitution types = 6, ncat = 4) corresponding to the best model selected (GTR + I + G) (Ronquist and Huelsenbeck, 2003), implemented using Markov Chain Monte Carlo simulations and four chains running for 3,000,000 generations. The first 25% of generations were discarded as burn-in.

Profiling of Bacterial Assemblages

Variations in the assemblage structure of both the DRB associated with the protists and the bacterioplankton in the culture medium (but outside the ciliate cells) among the treatments were assessed using terminal restriction fragment length polymorphism (T-RFLP). Bacterial 16S rRNA genes were amplified as described above, except that the forward primer 63F was labeled with a fluorescent dye, 6-carboxyfluorescein, at its 5′ end. The PCR products were purified with the TIAN Quick Midi Purification Kit (Tiangen, Beijing, China). The DNA yield was quantified using a NanoDrop 2000C spectrophotometer (Thermo Fisher, Wilmington, DE, United States). A 15 μL digestion mixture containing 7.5 μL of purified PCR product (each with about 20 ng of DNA) and 7.5 μL of digestion buffers with restriction endonuclease HhaI (Fermentas) were incubated at 37°C for 1 h. Sizes of the terminal restriction fragments (T-RFs) were determined using an ABI 3730 DNA analyzer (Sangon Biotech, Shanghai, China). The baseline threshold for signal detection was set to 50 fluorescence intensity units to eliminate any background interference. Only the peaks with T-RF lengths ranging from 40 to 400 bp were included in the subsequent analysis. The relative abundance of each T-RF was calculated as the peak area ratio of the T-RF to all T-RFs detected for a given sample. Minor peaks with a relative abundance of < 1% of the total were excluded, and the remaining peaks were presumed to represent bacterial phylotypes.

The assemblage information generated from the T-RFLP profiling was analyzed using the software package PRIMER v.6 (Primer-E, Plymouth, United Kingdom). In order to test the differences in DRB assemblages, relative abundances of T-RFs were log-transformed, and a matrix of assemblage similarities was generated using the Bray-Curtis index. Non-metric multidimensional scaling (MDS) was executed to visualize the differences in DRB assemblage structure among the treatments of each factor. To test the hypotheses that a given factor would affect the assemblage structure of the DRB and the bacterioplankton in the waters, analysis of similarity (ANOSIM) was performed.

RESULTS

Community Profiling of Bacterioplankton in the Culture Media

The T-RFLP profiling and ANOSIM results of global tests showed that all environmental factors investigated in this study, i.e., temperature ($R \geq 0.71$, $P \leq 0.014$), light ($R \geq 0.38$, $P \leq 0.039$), OTC ($R \geq 0.47$, $P = 0.001$), Pb ($R \geq 0.75$, $P \leq 0.002$), Hg ($R = 1.00$, $P = 0.001$), and Cd ($R = 0.76$, $P = 0.001$), significantly affected the community structure of bacterioplankton in the culture media for the tested ciliate species (**Table 1**). From the point view of the R statistic values of global tests, the effects of the tested heavy metals on the bacterioplankton community structure seem to be stronger than those of temperature, OTC antibiotics, and light.

Community Profiling of DRB

The DRB assemblages were clearly separated into three groups by temperature in *E. vannus*, which was well-illustrated in the MDS plots (**Figure 1B**), while the temperature-specific clusters somewhat overlapped in *P. bursaria* (**Figure 1A**). The analysis of the assemblage structure of the DRB generally showed similar results of the bacterioplankton, namely, the effects of temperature (global test, $R \geq 0.50$, $P = 0.001$), OTC ($R \geq 0.49$, $P = 0.001$), and Pb ($R \geq 0.80$, $P = 0.001$) were significant for the DRB in both species. Testing on a single species also illustrated that Hg ($R = 0.73$, $P = 0.001$) was an influential factor in the assemblage structure of DRB in *P. bursaria*, and Cd for that in *E. vannus* ($R = 0.79$, $P = 0.001$). The only exception was the light treatments in *P. bursaria*, in which the assemblage of DRB was not significantly different among the LL, LD, and DD treatments ($R = 0.05$, $P = 0.362$) (**Figure 1C** and **Table 1**).

The MDS plots showed that, within the same range of a given environmental factor, the DRB assemblages were clearly separated into three groups in the marine species but overlapped somewhat in the freshwater form (**Figure 1**). These patterns were also supported by the results of ANOSIM: the R-value of the DRB assemblage was consistently lower than that of the bacterioplankton community in all treatments of *P. bursaria* (i.e., $\Delta R_{mean} = R_{DRB} - R_{water} = -0.22$; $n = 5$) but higher in those of *E. vannus* (i.e., $\Delta R_{mean} = R_{DRB} - R_{water} = 0.15$; $n = 5$; **Table 1**). This indicated that the DRB assemblage was less variable in *P. bursaria* but more variable in *E. vannus* as compared with their surrounding bacterial prey under varying temperature, light, OTC, Pb, Hg, and Cd concentrations. The DRB and bacterioplankton community were also significantly different in a given treatment, especially under highly stressed conditions (e.g., at 25°C or in OTC20, see **Supplementary Table S1**).

Identity and Classification of Digestion-Resistant Bacteria

A total of 1018 raw sequences of 16S rRNA genes were obtained from 108 clone libraries and sequencing. After removing 110 chimeras, 908 remained (**Figure 2** and **Table 2**). Overall, most of these DRB belonged to the phylum Proteobacteria (61.3% for *P. bursaria* and 87.4% for *E. vannus*). The phylotypes belonging to Bacteroidetes (25.7%), Actinobacteria (13.8%),

TABLE 1 | Analysis of similarities (ANOSIM) statistics shows the differences in the community structures of digestion-resistant bacteria (DRB) in ciliates *Paramecium bursaria* and *Euplotes vannus*, as well as the bacterioplankton in their culture medium subjected to environmental changes.

Comparison	P. bursaria				E. vannus			
	Bacterioplankton		DRB		Bacterioplankton		DRB	
	R	*P*	*R*	*P*	*R*	*P*	*R*	*P*
Temperature (global test)	**0.77**	**0.014**	**0.50**	**0.001**	**0.71**	**0.004**	**0.86**	**0.001**
16°C vs. 21°C	0.04	0.400	0.15	0.071	0.96	0.100	**0.44**	**0.008**
21°C vs. 25°C	1.00	0.100	0.21	0.087	0.48	0.100	**1.00**	**0.008**
16°C vs. 25°C	1.00	0.100	0.11	0.127	0.93	0.100	**0.88**	**0.008**
Light (global test)	**0.41**	**0.014**	0.05	0.362	**0.38**	**0.039**	**0.87**	**0.001**
LL vs. DD	0.33	0.400	0.19	0.400	−0.30	0.900	**0.59**	**0.008**
LL vs. LD	0.56	0.100	0.33	0.300	0.89	0.100	**0.96**	**0.008**
DD vs. LD	0.33	0.400	0.00	0.700	0.52	0.100	**1.00**	**0.008**
OTC (global test)	**0.57**	**0.001**	**0.53**	**0.001**	**0.47**	**0.001**	**0.49**	**0.001**
OTC0 vs. OTC1	0.56	0.100	0.12	0.214	0.11	0.300	0.07	0.214
OTC0 vs. OTC10	0.56	0.100	**0.62**	**0.008**	0.67	0.100	0.17	0.103
OTC0 vs. OTC20	0.59	0.100	0.66	0.600	1.00	0.100	**0.35**	**0.008**
OTC1 vs. OTC10	0.93	0.100	0.05	0.706	0.30	0.100	**0.51**	**0.016**
OTC1 vs. OTC20	1.00	0.100	**0.23**	**0.048**	0.37	0.100	**0.52**	**0.016**
OTC10 vs. OTC20	-0.15	0.100	0.20	0.103	0.63	0.100	**0.32**	**0.016**
Pb^{2+} (global test)	**1.00**	**0.001**	**0.83**	**0.001**	**0.75**	**0.002**	**0.80**	**0.001**
Pb0 vs. Pb10	1.00	0.100	**0.63**	**0.029**	0.93	0.100	0.24	0.086
Pb0 vs. Pb30	1.00	0.100	**0.38**	**0.029**	0.56	0.100	**0.84**	**0.005**
Pb0 vs. Pb50	1.00	0.100	**0.56**	**0.029**	1.00	0.100	**0.46**	**0.005**
Pb10 vs. Pb30	1.00	0.100	0.42	0.057	0.70	0.200	1.00	**0.029**
Pb10 vs. Pb50	1.00	0.100	−0.01	0.486	0.59	0.100	0.40	0.057
Pb30 vs. Pb50	1.00	0.100	0.33	0.086	0.74	0.100	**0.71**	**0.029**
Hg^{2+} (global test)	**1.00**	**0.001**	**0.73**	**0.001**	–	–	–	–
Hg0 vs. Hg0.01	1.00	0.100	**0.25**	**0.029**	–	–	–	–
Hg0 vs. Hg0.05	1.00	0.100	**0.51**	**0.029**	–	–	–	–
Hg0 vs. Hg0.1	1.00	0.100	0.09	0.400	–	–	–	–
Hg0 vs. Hg0.05	1.00	0.100	−0.01	0.514	–	–	–	–
Hg0.01 vs. Hg0.1	1.00	0.100	0.16	0.057	–	–	–	–
Hg0.05 vs. Hg0.1	1.00	0.100	**0.42**	**0.029**	–	–	–	–
Cd^{2+} (global test)	–	–	–	–	**0.76**	**0.001**	**0.79**	**0.001**
Cd0 vs. Cd0.1	–	–	–	–	0.85	0.100	0.26	0.076
Cd0 vs. Cd0.5	–	–	–	–	0.52	0.100	0.25	0.114
Cd0 vs. Cd1	–	–	–	–	1.00	0.100	**0.85**	**0.005**
Cd0.1 vs. Cd0.5	–	–	–	–	0.63	0.100	0.02	0.429
Cd0.1 vs. Cd1	–	–	–	–	1.00	0.100	0.46	0.057
Cd0.5 vs. Cd1	–	–	–	–	1.00	0.100	**0.77**	**0.029**

Significant differences (P < 0.05) are highlighted in bold. Bacterial community differences are based on the Bray–Curtis dissimilarities. Consistently illuminated, completely dark, and 12 h:12 h alternation of light and dark conditions referred to as LL, DD and LD; oxytetracycline concentrations of 0, 1, 10, and 20 mg/L referred to as OTC0, OTC1, OTC10, and OTC20, respectively; lead concentrations of 0, 10, 30, and 50 mg/L referred to as Pb0, Pb10, Pb30, and Pb50, respectively; mercury concentrations of 0, 0.01, 0.05, and 0.1 mg/L referred to as Hg0, Hg0.01, Hg0.05, and Hg0.1, respectively; cadmium concentrations of 0, 0.1, 0.5, and 1 mg/L referred to as Cd0, Cd0.1, Cd0.5, and Cd1, respectively.

Verrucomicrobia (11.3%), and Firmicutes (0.53%) were relatively minor. The proteobacterial DRB belonged to proteobacterial classes (Gammaproteobacteria, Alphaproteobacteria, and Betaproteobacteria), of which Gammaproteobacteria was the most abundant in *P. bursaria* and *E. vannus*, accounting for 37.1 and 71.9%, respectively. The DRB of Alphaproteobacteria showed similar proportions in these two ciliates (10.3 and 13.4%), whereas the relative abundance of Betaproteobacteria

was much higher in the *P. bursaria* (13.8%) than in *E. vannus* (2.1%) (**Figure 2**).

A total of 84 OTUs were obtained for the DRB of these two ciliate species, of which 72 OTUs showed high sequence identity (97–100%) with described species, and the remaining 15 OTUs had sequence similarities lower than 97% (**Table 2**). The Proteobacteria OTUs were prevalent in the DRB assemblages of both ciliates, accounting for 81% of the OTUs observed (**Figure 2**
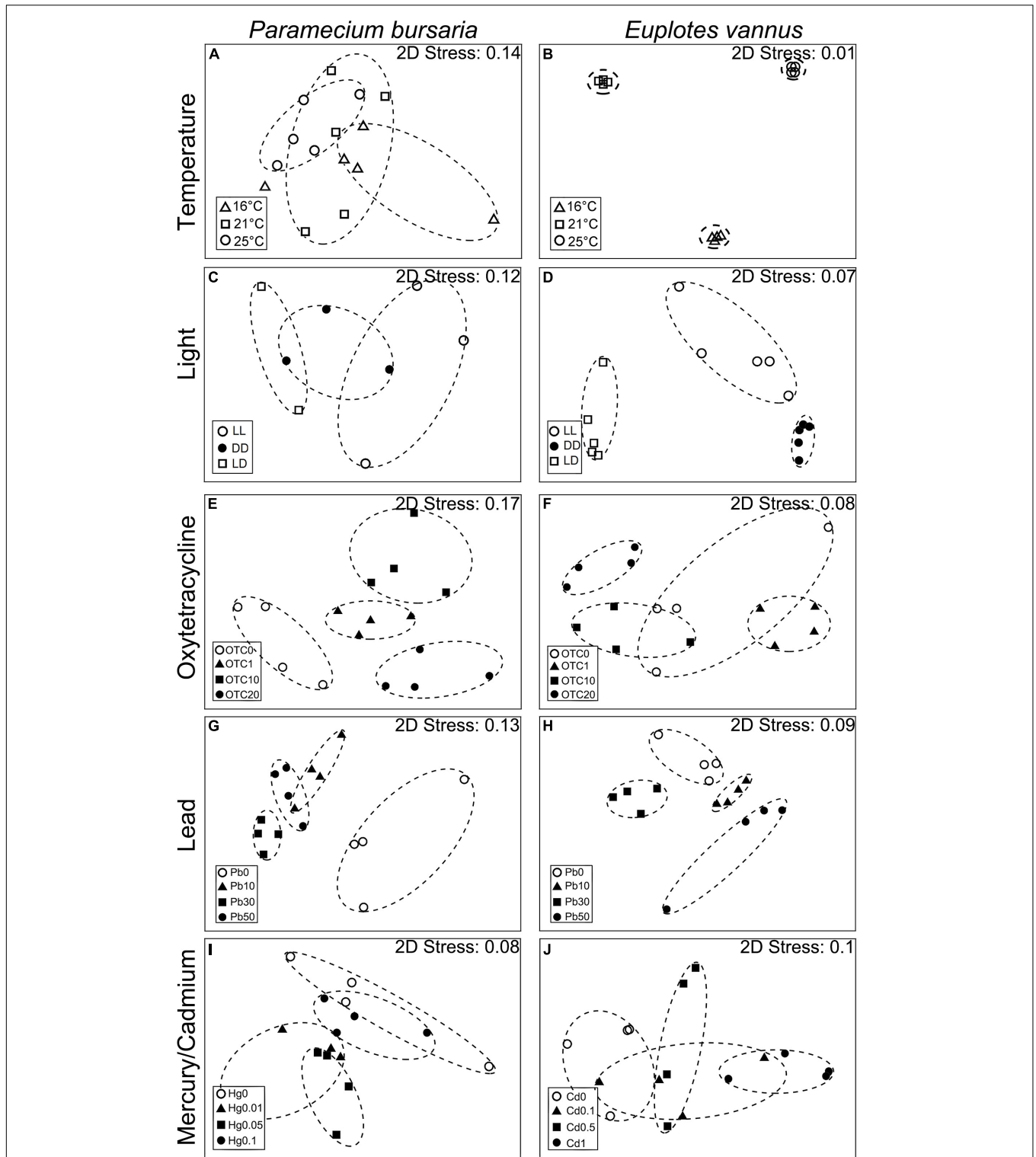
FIGURE 1 | Plots of multi-dimensional scaling ordinations based on Bray-Curtis similarities of the assembly of digestion-resistant bacteria (DRB) in the ciliates *Paramecium bursaria* **(A,C,E,G,I)** and *Euplotes vannus* **(B,D,F,H,J)** reared under different conditions. **(A,B)** At temperatures of 16°C, 21°C, and 25°C; **(C,D)** under three light conditions: consistently illuminated (LL), completely dark (DD), and diel light and dark cycles (LD); **(E,F)** under antibiotic treatments (OTC0, OTC1, OTC10, and OTC20) with the oxytetracycline concentrations of 0 mg/L (OTC0), 1 mg/L (OTC1), 10 mg/L (OTC10), and 20 mg/L (OTC20), respectively; **(G,H)** under lead treatments (Pb0, Pb10, Pb30, and Pb50) with the concentration of 0 mg/L (Pb0), 10 mg/L (Pb10), 30 mg/L (Pb30), and 50 mg/L (Pb50), respectively; **(I)** under mercury treatments (Hg0, Hg0.01, Hg0.05, and Hg0.1) for *P. bursaria* at 0 mg/L (Hg0), 0.01 mg/L (Hg0.01), 0.05 mg/L (Hg0.05), and 0.1 mg/L (Hg0.1), respectively; and **(J)** under cadmium treatments (Cd0, Cd0.1, Cd0.5, and Cd1) for *E. vannus* at 0 mg/L (Cd0), 0.1 mg/L (Cd0.1), 0.5 mg/L (Cd0.5), and 1 mg/L (Cd1), respectively.

FIGURE 2 | A pie chart showing the phylogenetic composition of digestion-resistant bacteria (DRB) in association with the ciliated protozoa *Paramecium bursaria* **(A)** and *Euplotes vannus* **(B)**.
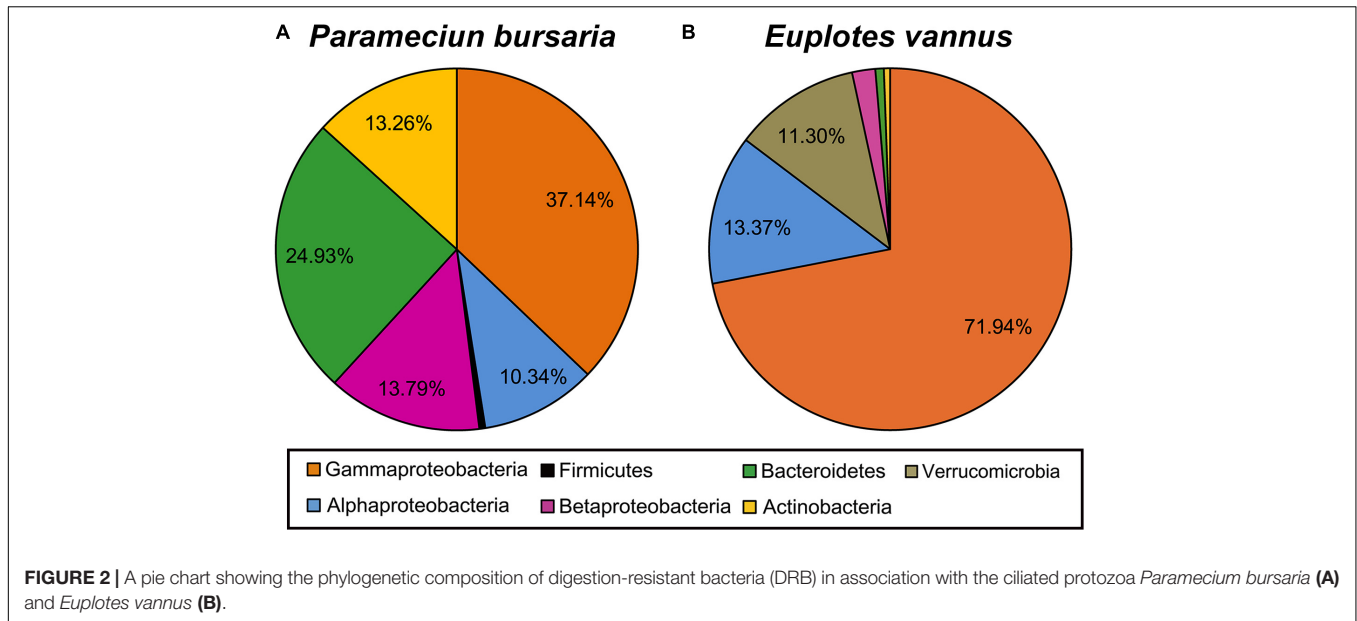
and **Table 2**). Gammaproteobacteria (41) also dominated in terms of OTU number, which was about three times the amount of Alphaproteobacteria (14) and Betaproteobacteria (13).

A majority of Gammaproteobacteria OTUs were mostly affiliated with the genera *Pseudoalteromonas* (13 OTUs), *Aestuariibacter* (5 OTUs), *Alteromonas* (5 OTUs), and *Pseudomonas* (5 OTUs). The phylotypes of the former three genera were exclusively detected in the marine ciliate *E. vannus*, whereas the phylotypes of *Pseudomonas* were detected in the DRB assemblages of *both P. bursaria* and *E. vannus* (**Table 2**). *Nevskia* (2 OTUs) and *Spongiibacter* (2 OTUs) had fewer OTUs, and *Aeromonas*, *Acinetobacter*, *Alcanivorax*, *Escherichia*, *Haemophilus*, *Psychrosphaera*, *Serratia*, and *Vibrio* were each represented with a single OTU (**Table 2**).

The most frequently occurring OTUs from DRB in the Alphaproteobacteria were affiliated with the family *Rhodobacteraceae* (5 OTUs, with five genera *Thalassococcus, Nautella, Ruegeria, Paracoccus*, and *Sulfitobacter*) (**Table 2**). The phylotypes of the family *Caulobacteraceae* were represented by 4 OTUs and two genera, *Caulobacter* and *Asticcacaulis*, which were abundant in the DRB assemblages of *P. bursaria* under the light treatments (**Table 2**). Two OTUs belonged to the genus *Sphingomonas* and occurred in both ciliates. The remaining three alphaproteobacterial OTUs were *Methylobacterium*, *Phyllobacterium*, and *Agrobacterium,* which were all associated with the *P. bursaria*. Nearly all of the Betaproteobacteria OTUs were recovered from *P. bursaria*, except for one OTU (*Pelomonas* sp.) detected in both two ciliate species (**Table 2**). Other OTUs were affiliated with the genera *Aquabacterium*, *Curvibacter*, *Hydrogenophaga*, *Janthinobacterium*, *Methylophilus*, *Polynucleobacter*, *Limnobacter*, *Ralstonia*, and *Variovorax* (**Table 2**).

There were 10 OTUs of DRB affiliated with the phylum Bacteroidetes. These included two OTUs of *Arcicella* and another two of *Flectobacillus*, both of which are members of the family

Cytophagaceae (**Table 2**). Three OTUs of *Flavobacteriaceae* were closely related to *Ochrovirga* and *Flavobacterium*. Two OTUs were members of *Cryomorphaceae*: one was affiliated with *Fluviicola,* and the other could represent a new genus within this family (**Figure 3A**), exhibiting a 90% similarity with the 16S rRNA gene of *Vicingus serpentipes* (**Table 2**). The OTU sharing an 88% sequence similarity with *Crocinitomix catalasitica* was confirmed to be a member of the order Flavobacteriales but remained unresolved at the family level in the ML and Bayesian trees (**Figure 3A**). The remaining OTU of this phylum was closely related to *Algoriphagus* (**Table 2**).

The actinobacterial DRB were represented by two OTUs affiliated with *Micrococcus* and *Propionibacterium* (**Table 2**). Another two OTUs were related to *Anaerocolumna* and *Peptoniphilus* (phylum Firmicutes), which were only detected in the freshwater ciliate (**Table 2**). A single verrucomicrobial OTU, which was associated with the marine ciliate *E. vannus*, shared a low sequence similarity (89%) with *Ruficoccus amylovorans* (family *Puniceicoccaceae*), likely representing a new genus (**Figure 3B** and **Table 2**).

Warming Effect on the Assemblage Structure of DRB

Analysis of the clone libraries indicated that the DRB assemblage in *P. bursaria* was dominated by *Pseudomonas* spp., of which the relative abundance gradually increased from 50% to 65% and 76% with increasing temperature (**Table 2** and **Figure 4A**). *Flavobacterium*, *Peptoniphilus*, and *Micrococcus*, though not abundant, were only detected in the warmest treatment for the freshwater ciliate. In contrast, the DRB assemblage in *E. vannus* was generally dominated by *Pseudoalteromonas* spp., of which the relative abundance decreased from 74% to 40% with temperature. The relative abundance of *Vibrio* sp. was minor (2.7%) during the treatment at 16°C but became abundant (50%) at 25°C (**Table 2**

TABLE 2 | Detection and classification of digestion-resistant bacteria (DRB) in *Paramecium bursaria* (P) and *Euplotes vannus* (E) in various temperature, light, antibiotic, and heavy metal treatments.

OTU ID	Accession number	Closest matched species (accession number)	Coverage (%)	Identity (%)	Classification	Treatment	Ciliate
OTU1	MH556452	*Aestuariibacter* sp. strain 12C24 (KU963301)	100	99–100	*Gamma, Alteromonadaceae*	25°C; LD; OTC0, OTC1, OTC10; Pb10, Pb30, Pb50; Cd0, Cd0.1, Cd0.5, Cd1.0	E
OTU2	MH556787	*Aestuariibacter halophilus* (LC221844)	100	99	*Gamma, Alteromonadaceae*	LD; OTC1, OTC20	E
OTU3	MH556783	*Aestuariibacter* sp. Bh22 (LN897328)	100	94	*Gamma, Alteromonadaceae*	OTC20	E
OTU4	MH556703	*Aestuariibacter aggregatus* strain WH169 (MH414455)	100	97	*Gamma, Alteromonadaceae*	OTC20	E
OTU5	MH556467	*Aestuariibacter* sp. strain 12C24 (KU963301)	100	97–98	*Gamma, Alteromonadaceae*	OTC0; Cd0.1	E
OTU6	MH556726	*Alteromonas* sp. H86 (FJ903192)	100	98	*Gamma, Alteromonadaceae*	OTC1	E
OTU7	MH556162	*Alteromonas* sp. M71_D24 (FM992713)	100	95	*Gamma, Alteromonadaceae*	LD	E
OTU8	MH556150	*Alteromonas* sp. SPB-8 (DQ412077)	93	98	*Gamma, Alteromonadaceae*	LD	E
OTU9	MH556135	*Alteromonas* sp. AKA07-1 (AB571941)	100	97–98	*Gamma, Alteromonadaceae*	LD; OTC0, OTC1	E
OTU10	MH556153	*Alteromonas tagae* strain BCRC 17571 (NR_043977)	100	97–99	*Gamma, Alteromonadaceae*	LD, LL	E
OTU11	MH556079	*Pseudoalteromonas phenolica* strain JCM 21460 (NR_113299)	100	96–97	*Gamma, Pseudoalteromonadaceae*	LL, DD	E
OTU12	MH556080	*Pseudoalteromonas* sp. 03/034 (AJ874351)	100	96–98	*Gamma, Pseudoalteromonadaceae*	LL	E
OTU13	MH556095	*Psychrosphaera saromensis* strain DL8-2 (KF146527)	100	97–98	*Gamma, Pseudoalteromonadaceae*	LL, DD, LD	E
OTU14	MH556118	*Pseudoalteromonas* sp. 03/034 (AJ874351)	100	99	*Gamma, Pseudoalteromonadaceae*	16°C; DD, LL	E
OTU15	MH556233	*Pseudoalteromonas piscicida* strain MCCB 201 (KF880965)	100	98–99	*Gamma, Pseudoalteromonadaceae*	25°C	E
OTU16	MH556167	*Pseudoalteromonas* sp. 01/121 (AJ874345)	100	98–100	*Gamma, Pseudoalteromonadaceae*	16°C, 21°C; DD, LL	E
OTU17	MH556181	*Pseudoalteromonas* sp. A28 (AF227238)	100	95	*Gamma, Pseudoalteromonadaceae*	16°C	E
OTU18	MH556191	*Pseudoalteromonas* sp. BSw21650 (JF697294)	100	98–99	*Gamma, Pseudoalteromonadaceae*	16°C, 21°C	E
OTU19	MH556216	*Pseudoalteromonas* sp. CF6-1 (FJ169996)	100	96	*Gamma, Pseudoalteromonadaceae*	21°C	E
OTU20	MH556254	*Pseudoalteromonas* sp. HK41 (HQ343275)	100	97–98	*Gamma, Pseudoalteromonadaceae*	25°C	E
OTU21	MH556169	*Pseudoalteromonas* sp. KASP34 (KU647930)	99	99	*Gamma, Pseudoalteromonadaceae*	16°C	E
OTU22	MH556210	*Pseudoalteromonas* sp. S1649 (FJ457154)	100	98–99	*Gamma, Pseudoalteromonadaceae*	16°C, 21°C; LL, DD	E
OTU23	MH556188	*Pseudoalteromonas* sp. S511-1 (AB029824)	100	97–98	*Gamma, Pseudoalteromonadaceae*	16°C, 21°C	E
OTU24	MH556236	*Pseudoalteromonas viridis* (AB681561)	100	95	*Gamma, Pseudoalteromonadaceae*	25°C	E
OTU25	MH556186	*Algicola bacteriolytica* strain MR32e (HQ439519)	99	95	*Gamma, Pseudoalteromonadaceae*	16°C	E
OTU26	MH555990	*Pseudomonas synxantha* strain NBRC 3913 (NR_113583)	100	98–99	*Gamma, Pseudomonadaceae*	16°C; OTC1	E, P
OTU27	MH555987	*Pseudomonas psychrophila* strain P270 (KC904093)	100	99–100	*Gamma, Pseudomonadaceae*	16°C, 21°C, 25°C; OTC1, OTC10, OTC20	P

(Continued)

TABLE 2 | Continued

OTU ID	Accession number	Closest matched species (accession number)	Coverage (%)	Identity (%)	Classification	Treatment	Ciliate
OTU28	MH556036	*Pseudomonas* sp. K3R3.1A (KC433646)	100	99	*Gamma, Pseudomonadaceae*	21°C, 25°C; Hg0.01; OTC0, OTC10, OTC20	P
OTU29	MH556031	*Pseudomonas fluorescens* strain ex17 (KF317887)	100	99–100	*Gamma, Pseudomonadaceae*	16°C, 21°C, 25°C; OTC0, OTC1, OTC10; Pb10; Hg0, Hg0.01, Hg0.1	E, P
OTU30	MH556663	*Pseudomonas* sp. R02 (KT890300)	100	98	*Gamma, Pseudomonadaceae*	OTC20	P
OTU31	MH555949	*Nevskia ramosa* strain Soe1 (NR_025269)	99	98–99	*Gamma, Sinobacteraceae*	DD, LD, LL	P
OTU32	MH555974	*Nevskia ramosa* (AJ001343)	99	95	*Gamma, Sinobacteraceae*	DD	P
OTU33	MH556800	*Spongiibacter marinus* (AB985586)	100	96–97	*Gamma, Spongiibacteraceae*	OTC10	E
OTU34	MH556747	*Spongiibacter marinus* (AB985580)	100	99	*Gamma, Spongiibacteraceae*	OTC10, OTC20; LD	E
OTU35	MH556281	*Escherichia coli* strain Y38 (JN578647)	100	99	*Gamma, Enterobacteriaceae*	Hg0, Hg0.05, Hg0.1	P
OTU36	MH556409	*Serratia proteamaculans* strain PW172 (JF494823)	100	99	*Gamma, Enterobacteriaceae*	Pb50	P
OTU37	MH556249	*Vibrio neocaledonicus* strain MS1 (KJ841877)	100	99	*Gamma, Vibrionaceae*	16°C, 25°C	E
OTU38	MH556000	*Aeromonas caviae* strain AH08 (KU975030)	100	99	*Gamma, Aeromonadaceae*	16°C	P
OTU39	MH556788	*Alcanivorax* sp. MCCC 1A00973 (KU681505)	100	99	*Gamma, Alcanivoracaceae*	OTC20	E
OTU40	MH556230	*Acinetobacter junii* strain B2w (KX058411)	100	99	*Gamma, Moraxellaceae*	21°C; LD; Hg0.01, Hg0.05; OTC0, OTC10	E, P
OTU41	MH556303	*Haemophilus* sp. oral (AY005034)	100	99	*Gamma, Pasteurellaceae*	Hg0.01	P
OTU42	MH556285	*Asticcacaulis excentricus* strain CB 48 (NR_114730)	98–100	99	*Alpha, Caulobacteraceae*	Hg0, Hg0.1	P
OTU43	MH555955	*Asticcacaulis* sp. clone Sa4_4.4 (GQ181156)	100	98	*Alpha, Caulobacteraceae*	LD, DD, LL	P
OTU44	MH555978	*Caulobacter* sp. BBCT11 (DQ337547)	100	96	*Alpha, Caulobacteraceae*	DD	P
OTU45	MH555956	*Caulobacter* sp. DNA (AJ227760)	100	99	*Alpha, Caulobacteraceae*	LL	P
OTU46	MH556716	*Thalassococcus* sp. KU27F5 (AB636146)	100	99	*Alpha, Rhodobacteraceae*	OTC1	E
OTU47	MH556768	*Nautella* sp. A04V (LC094988)	100	97–99	*Alpha, Rhodobacteraceae*	LL; OTC0, OTC1, OTC10	E
OTU48	MH556144	*Ruegeria pelagia* strain NBRC 102038 (NR_114024)	100	99–100	*Alpha, Rhodobacteraceae*	LL, LD	E
OTU49	MH556262	*Paracoccus* sp. I7 (KR108387)	100	99	*Alpha, Rhodobacteraceae*	Hg0	P
OTU50	MH556666	*Sulfitobacter* sp. QD214-NF102 (KC689801)	100	99	*Alpha, Rhodobacteraceae*	OTC20	P
OTU51	MH555995	*Sphingomonas abaci* strain SS1-08 (KU341393)	100	99	*Alpha, Sphingomonadaceae*	LD; 16°C; OTC0, OTC1, OTC10, OTC20	E, P
OTU52	MH556759	*Sphingomonas roseiflava* strain MK341 (NR_117716)	100	97	*Alpha, Sphingomonadaceae*	OTC10	E
OTU53	MH556325	*Methylobacterium* sp. 20 (JF905619)	100	99	*Alpha, Methylobacteriaceae*	Hg0.05	P
OTU54	MH556314	*Phyllobacterium myrsinacearum* isolate OTU-a22 (KJ147062)	100	99	*Alpha, Phyllobacteriaceae*	16°C; Hg0.05	P

(Continued)

TABLE 2 | Continued

OTU ID	Accession number	Closest matched species (accession number)	Coverage (%)	Identity (%)	Classification	Treatment	Ciliate
OTU55	MH556037	*Agrobacterium rhizogenes* strain IV (HM582866)	100	99	*Alpha, Rhizobiaceae*	21°C	P
OTU56	MH556569	*Pelomonas* sp. clone 35Fe00 (KF287732)	100	99	*Beta, Comamonadaceae*	Pb30, Pb50; Hg0.01; Cd0.1, Cd1.0	E, P
OTU57	MH556333	*Hydrogenophaga* sp. 7B-224 (KF441666)	99	98	*Beta, Comamonadaceae*	Hg0.1	P
OTU58	MH555972	*Curvibacter lanceolatus* strain NBRC 103051 (NR_114201)	100	98–99	*Beta, Comamonadaceae*	LL, LD, DD	P
OTU59	MH555959	*Variovorax paradoxus* (HQ845986)	100	99	*Beta, Comamonadaceae*	LL, LD	P
OTU60	MH556621	*Ralstonia* sp. S1SM82 (KT183537)	100	99	*Beta, Burkholderiaceae*	OTC0	P
OTU61	MH556271	*Polynucleobacter acidiphobus* (AB599874)	100	99	*Beta, Burkholderiaceae*	Hg0	P
OTU62	MH556312	*Limnobacter* sp. KNF002 (AB426551)	100	99	*Beta, Burkholderiaceae*	Hg0.05	P
OTU63	MH556310	*Aquabacterium commune* strain B8 (NR_024875)	100	98–99	*Beta, Burkholderiales*	Hg0.01, Hg0.05	P
OTU64	MH556265	*Aquabacterium fontiphilum* strain K10 (KT345664)	100	99	*Beta, Burkholderiales*	Hg0	P
OTU65	MH556313	*Aquabacterium fontiphilum* strain CS-6 (NR_044322)	98	98	*Beta, Burkholderiales*	Hg0.05	P
OTU66	MH556272	*Limnobacter* sp. strain DRY11W (MH463959)	100	94	*Beta, Burkholderiales*	Hg0	P
OTU67	MH556266	*Methylophilus methylotrophus* strain NCIMB 10515 (NR_041257)	99	99	*Beta, Methylophilaceae*	Hg0	P
OTU68	MH556063	*Janthinobacterium* sp. TP-Snow-C76 (KC987006)	100	99	*Beta, Oxalobacteraceae*	16°C, 25°C	P
OTU69	MH556619	*Arcicella aquatica* strain NO-502 (NR_029000)	100	99	*Bacteroidetes, Cytophagaceae*	OTC0	P
OTU70	MH556411	*Arcicella rigui* strain HMF3820 (KT983986)	100	96	*Bacteroidetes, Cytophagaceae*	Pb50	P
OTU71	MH556371	*Flectobacillus* sp. WG3 (FN547417)	100	98–99	*Bacteroidetes, Cytophagaceae*	Pb10, Pb30, Pb50; Hg0, Hg0.05	P
OTU72	MH556345	*Flectobacillus rhizosphaerae* strain JC289 (NR_137382)	96	95	*Bacteroidetes, Cytophagaceae*	Pb10	P
OTU73	MH556228	*Ochrovirga pacifica* (JN596241)	97	95	*Bacteroidetes, Flavobacteriaceae*	21°C	E
OTU74	MH556330	*Flavobacterium fontis* strain MIC3010 (NR_109522)	96	99	*Bacteroidetes, Flavobacteriaceae*	Hg0.1	P
OTU75	MH556040	*Flavobacterium* sp. T3L.05.LWF.W.Kidney.D (JX287789)	98	99–100	*Bacteroidetes, Flavobacteriaceae*	25°C	P
OTU76	MH556400	*Fluviicola hefeinensis* strain MYL-8 (NR_133750)	100	98	*Bacteroidetes, Cryomorphaceae*	Pb50	P
OTU77	MH556320	*Vicingus serpentipes* strain ANORD5 (NR_159281)	100	90	*Bacteroidetes, Cryomorphaceae*	Hg0.05	P

(Continued)

TABLE 2 | Continued

OTU ID	Accession number	Closest matched species (accession number)	Coverage (%)	Identity (%)	Classification	Treatment	Ciliate
OTU78	MH556294	Algoriphagus aquatilis strain NBRC 104237 (NR_114262)	100	99	Bacteroidetes, Cyclobacteriaceae	Hg0.01	P
OTU79	MH556315	Crocinitomix catalasitica IFO 15977 (NR_040905)	95	88	Bacteroidetes	Hg0.05	P
OTU80	MH556064	Micrococcus sp. ce2 (JN082244)	99	99	Actino, Micrococcaceae	25°C	P
OTU81	MH556002	Propionibacterium acnes strain ChDC KB81 (KF933807)	99	99	Actino, Propionibacteriaceae	LD; 16°C, 21°C, 25°C; Hg0; Pb50	E, P
OTU82	MH556282	Anaerocolumna sp. CBA3638 (CP048000)	99	93	Firmicutes, Lachnospiraceae	Hg0	P
OTU83	MH556048	Peptoniphilus sp. EL1 (LN867000)	99	99	Firmicutes, Peptoniphilaceae	25°C	P
OTU84	MH556212	Ruficoccus amylovorans CC-MHH0563 (NR_156844)	99	89	Verrucomicrobia, Puniceicoccaceae	16°C, 21°C, 25°C; LD;OTC0, OTC1, OTC10; Cd0, Cd0.1, Cd0.5	E

Notes: Consistently illuminated, completely dark, and 12 h:12 h alternation of light and dark conditions referred to as LL, DD and LD; oxytetracycline concentrations of 0, 1, 10, and 20 mg/L referred to as OTC0, OTC1, OTC10, and OTC20, respectively; lead concentrations of 0, 10, 30, and 50 mg/L referred to as Pb0, Pb10, Pb30, and Pb50, respectively; mercury concentrations of 0, 0.01, 0.05, and 0.1 mg/L referred to as Hg0, Hg0.01, Hg0.05, and Hg0.1, respectively; cadmium concentrations of 0, 0.1, 0.5, and 1 mg/L referred to as Cd0, Cd0.1, Cd0.5, and Cd1, respectively.

and **Figure 4A**). *Ruficoccus*-like species (Verrucomicrobia) were consistently present, accounting for a small portion (3.3–13.5%) of the DRB in association with *E. vannus*. Nevertheless, warming induced a gradual decrease in its relative abundance. *Aestuariibacter* and *Pseudomonas* spp. were present only in the warmest treatment of the *Euplotes* (**Figure 4A**).

Variations in the Bacterial Assemblages Under Photoperiod Conditions

E. vannus under the condition of LD hosted 9 bacterial genera, which was much more diverse than that in both LL and DD. Structurally, *Pseudoalteromonas* spp. and *Psychrosphaera saromensis* dominated under conditions of both LL and DD, whereas *Aestuariibacter* spp. were the most abundant (31%) in the LD treatment. Phylotypes of *Aestuariibacter*, *Propionibacterium*, *Sphingomonas*, *Spongiibacter*, and *Ruficoccus*-like were detected only under the LD treatment (**Figure 4B**). In contrast, *P. bursaria* consistently hosted *Nevskia* sp. (38–44%), *Curvibacter* (25–29%), and *Asticcacaulis* (6–25%). Interestingly, *Caulobacter* and *Variovorax* were present but not in LD and DD, respectively (**Figure 4B**).

## Bacteria Co-resistant to Antibiotic and Digestion

Sphingomonas and *Arcicella* species occurred in the DRB of *P. bursaria*, accounting for 73% in the control (OTC0). However, these two taxa were not detectable in the OTC treatments. *Pseudomonas* in the control *P. bursaria* had a low abundance (19%) but a high abundance (50%–100%) after OTC applications. Also, *Sulfitobacter* was absent in the control and at a lower dose of OTC but represented 47% of the DRB in the OTC20 treatment (**Figure 5A**).

The bacteria associated with *E. vannus* treated with OTC included *Aestuariibacter*, *Acinetobacter*, *Alcanivorax*, *Alteromonas*, *Pseudomonas*, *Nautella*, *Thalassococcus*, *Sphingomonas*, *Spongiibacter*, and *Ruficoccus*-like Verrucomicrobia (**Figure 5A**). In contrast to the non-detection of *Sphingomonas* in *P. bursaria* at high doses of OTC, this genus occurred with high relative abundance in *E. vannus* treated with 10 and 20 mg/L of OTC. Both the *Aestuariibacter* and *Ruficoccus*-like phylotypes were abundant at the low-dose treatment but were reduced or disappeared at the higher doses (**Figure 5A**).

DRB Assemblages Changed With the Concentrations of Heavy Metals

The DRB in the control *P. bursaria* (Pb0) were represented by nine bacterial genera, of which only four were detected in the Pb-treated treatments, including *Flectobacillus*, *Pseudomonas*, *Fluviicola*, and *Serratia*. *Flectobacillus* was the most dominant, accounting for 83%, 100%, and 64% in Pb10, Pb30, and Pb50, respectively. *Fluviicola* and *Serratia* together represented 36% sequences in Pb50 (**Table 2** and **Figure 5B**).

There were many DRB persisting in the Hg treatments. These included *Acinetobacter*, *Aquabacterium*, *Escherichia*, *Flavobacterium*, *Hydrogenophaga*, *Pelomonas*, *Phyllobacterium*, and *Pseudomonas*. The most abundant at the high dose
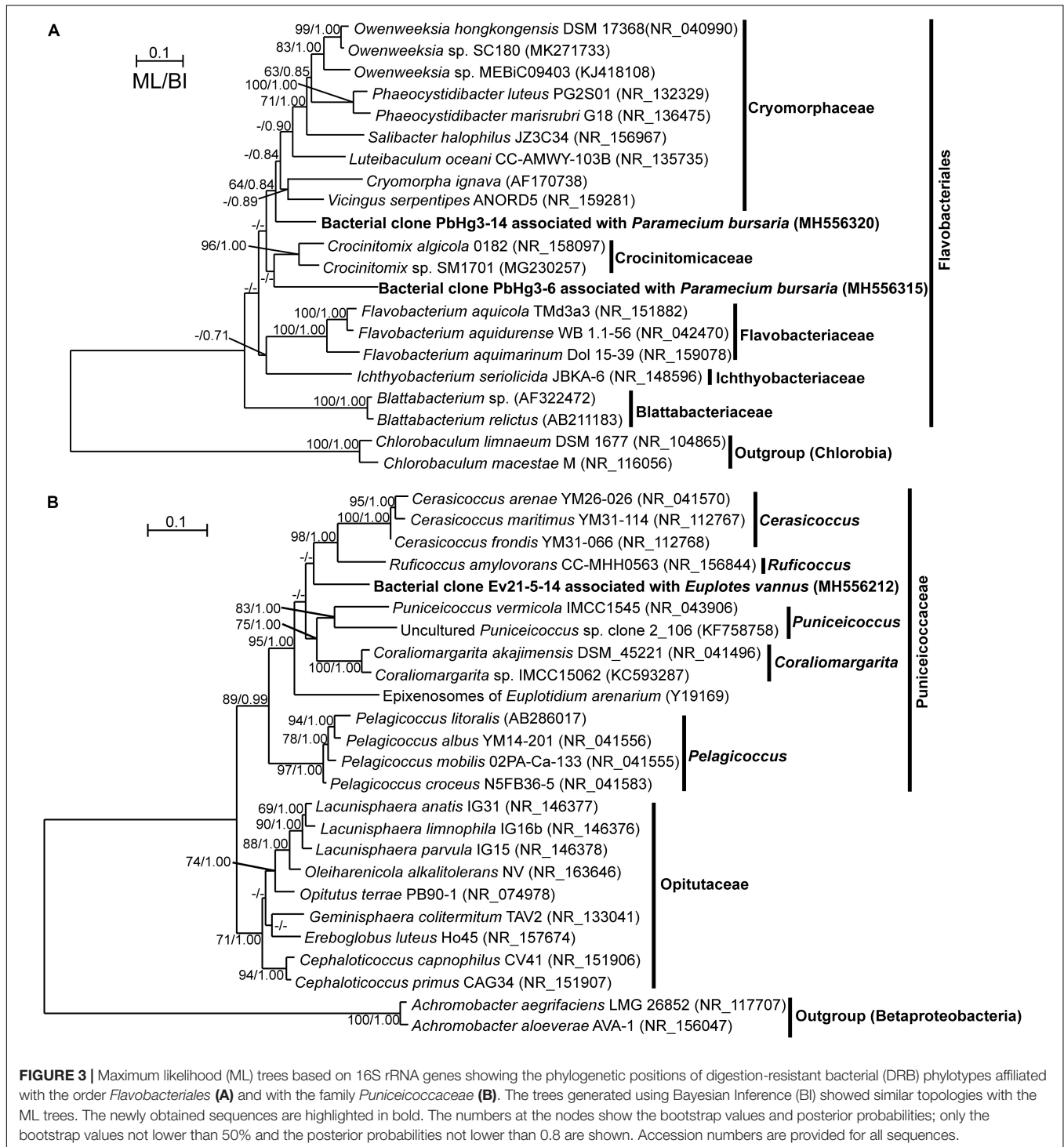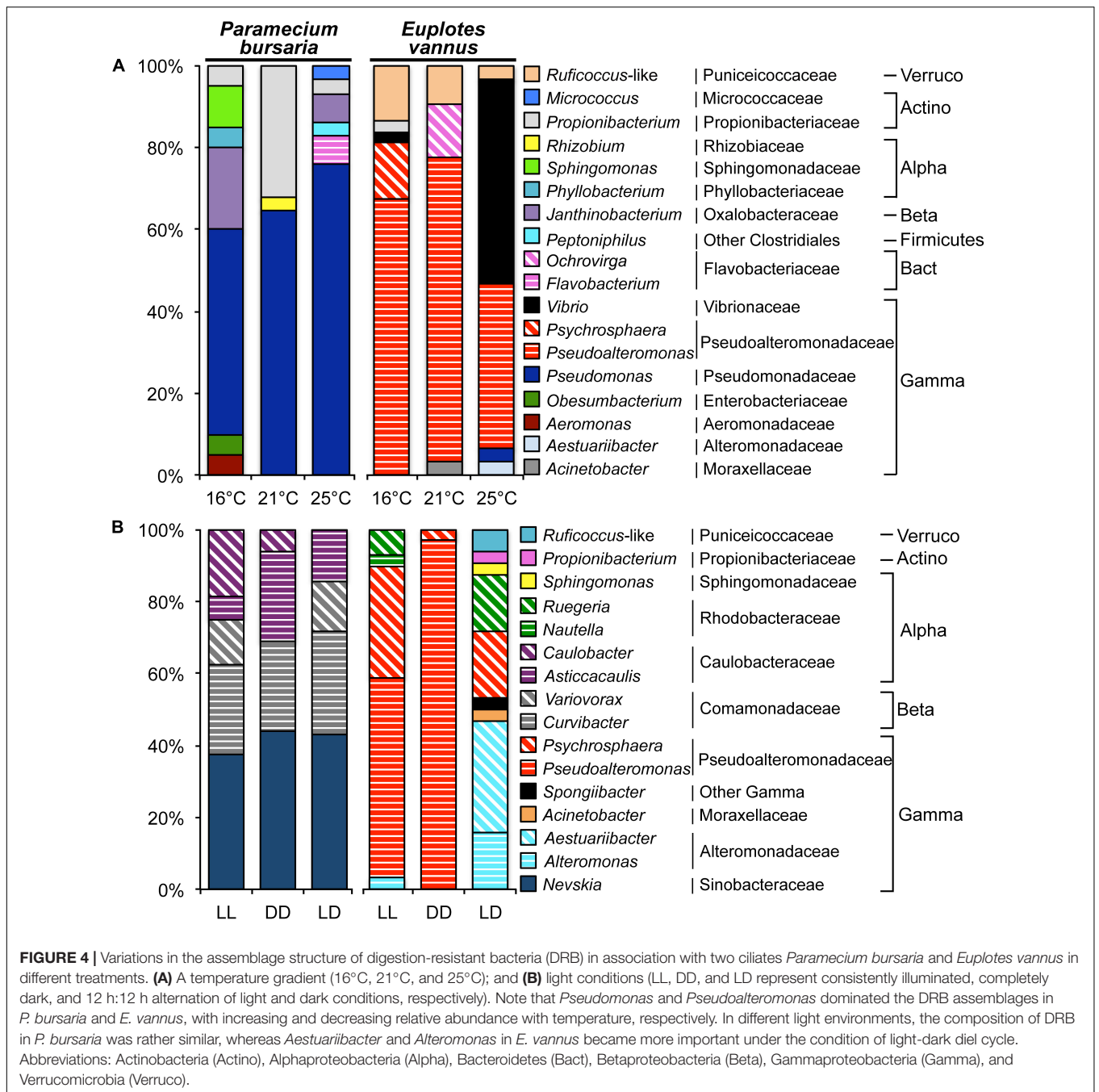
FIGURE 3 | Maximum likelihood (ML) trees based on 16S rRNA genes showing the phylogenetic positions of digestion-resistant bacterial (DRB) phylotypes affiliated with the order *Flavobacteriales* **(A)** and with the family *Puniceicoccaceae* **(B)**. The trees generated using Bayesian Inference (BI) showed similar topologies with the ML trees. The newly obtained sequences are highlighted in bold. The numbers at the nodes show the bootstrap values and posterior probabilities; only the bootstrap values not lower than 50% and the posterior probabilities not lower than 0.8 are shown. Accession numbers are provided for all sequences.

of HgCl$_2$ were *Hydrogenophaga* (42%) and *Escherichia* (25%), whereas *Acinetobacter* (54%) and *Pseudomonas* (13%) dominated the assemblage in the low dose treatment (**Table 2** and **Figure 5C**).

The DRB assemblage in *E. vannus* was consistently dominated by a single genus, *Aestuariibacter*, in both Pb and Cd treatments (**Table 2** and **Figures 5B,C**). Nevertheless,

Pelomonas (11%) occurred in Pb30 and increased to 17% in Pb50 (**Figure 5B**). Furthermore, in the treatments of Cd0.1 and Cd1.0, *Pelomonas* was also present but with minor proportions (3 and 8%, respectively). *Ruficoccus*-like Verrucomicrobia was minor (3.6%) in the control but abundant (~35%) in both Cd0.1 and Cd0.5 treatments (**Table 2** and **Figure 5C**).

FIGURE 4 | Variations in the assemblage structure of digestion-resistant bacteria (DRB) in association with two ciliates *Paramecium bursaria* and *Euplotes vannus* in different treatments. **(A)** A temperature gradient (16°C, 21°C, and 25°C); and **(B)** light conditions (LL, DD, and LD represent consistently illuminated, completely dark, and 12 h:12 h alternation of light and dark conditions, respectively). Note that *Pseudomonas* and *Pseudoalteromonas* dominated the DRB assemblages in *P. bursaria* and *E. vannus*, with increasing and decreasing relative abundance with temperature, respectively. In different light environments, the composition of DRB in *P. bursaria* was rather similar, whereas *Aestuariibacter* and *Alteromonas* in *E. vannus* became more important under the condition of light-dark diel cycle. Abbreviations: Actinobacteria (Actino), Alphaproteobacteria (Alpha), Bacteroidetes (Bact), Betaproteobacteria (Beta), Gammaproteobacteria (Gamma), and Verrucomicrobia (Verruco).
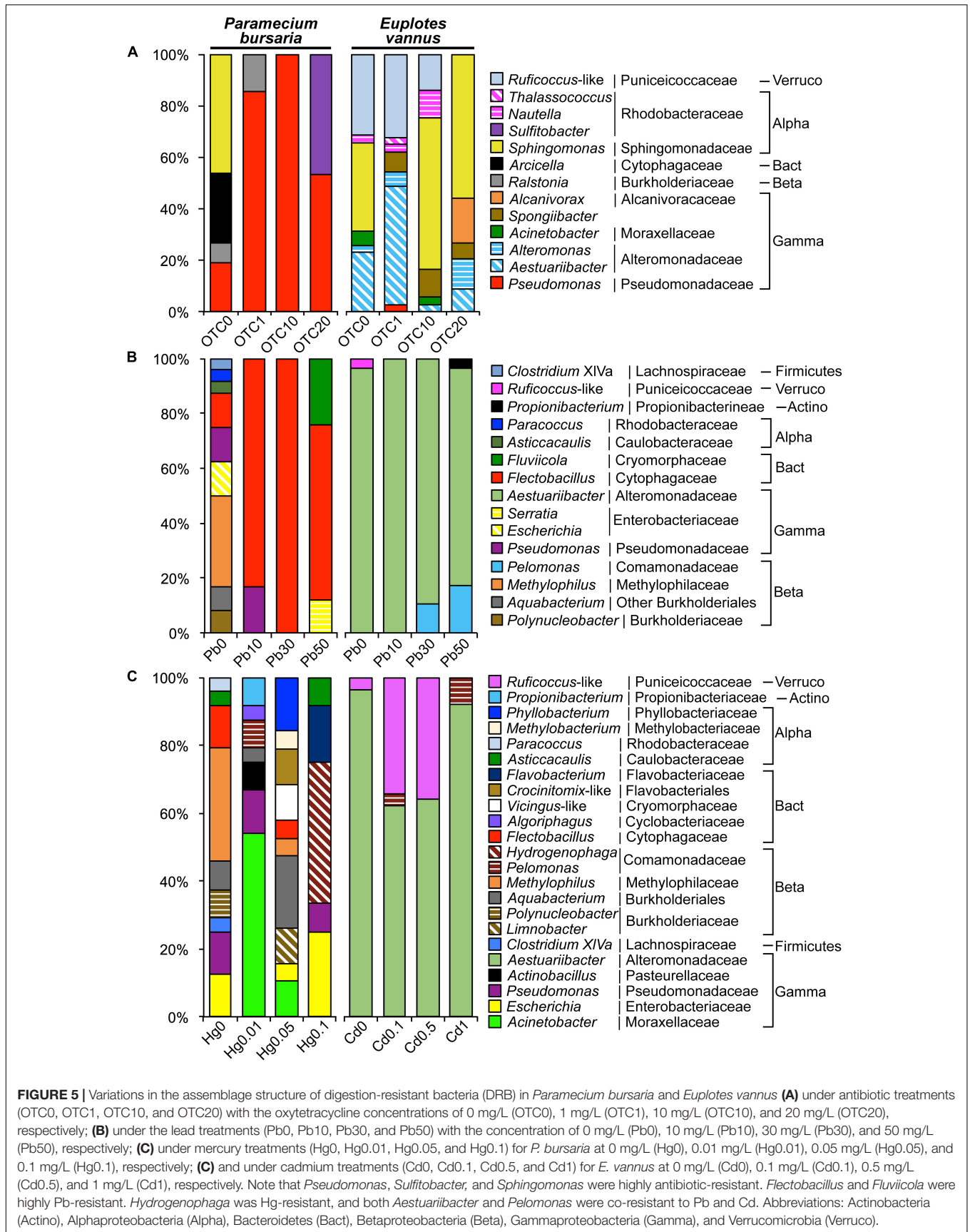
DISCUSSION

By using *E. vannus* and *P. bursaria* as models, this study is the first to explicitly investigate how the composition and structure of DRB assemblages vary along various physical and chemical gradients. Overall, our molecular profiling of these two protist species indicated that experimentally manipulated warming, irradiance, antibiotic, and heavy metal stresses significantly influenced the structure of DRB assemblages. This provides evidence that the association between DRB and protists is highly dependent on environmental conditions.

It was conceivable that there were consistently larger variations in the assemblage structure of DRB, relative to those in the environmental bacterioplankton across the treatments of *E. vannus* (**Table 1**). This is likely related to the fact that the variations in the environmental factors caused the shifts in the bacterioplankton community structure first (**Supplementary Table S1**), and then selective ingestion and differential digestion of the engulfed bacterial taxa took place next, which further screened out digestible populations, resulting in the altered assemblage structure of the bacteria (i.e., DRB) that resided in the protistan cells (**Table 1** and **Figures 4, 5**). However,

FIGURE 5 | Variations in the assemblage structure of digestion-resistant bacteria (DRB) in *Paramecium bursaria* and *Euplotes vannus* **(A)** under antibiotic treatments (OTC0, OTC1, OTC10, and OTC20) with the oxytetracycline concentrations of 0 mg/L (OTC0), 1 mg/L (OTC1), 10 mg/L (OTC10), and 20 mg/L (OTC20), respectively; **(B)** under the lead treatments (Pb0, Pb10, Pb30, and Pb50) with the concentration of 0 mg/L (Pb0), 10 mg/L (Pb10), 30 mg/L (Pb30), and 50 mg/L (Pb50), respectively; **(C)** under mercury treatments (Hg0, Hg0.01, Hg0.05, and Hg0.1) for *P. bursaria* at 0 mg/L (Hg0), 0.01 mg/L (Hg0.01), 0.05 mg/L (Hg0.05), and 0.1 mg/L (Hg0.1), respectively; **(C)** and under cadmium treatments (Cd0, Cd0.1, Cd0.5, and Cd1) for *E. vannus* at 0 mg/L (Cd0), 0.1 mg/L (Cd0.1), 0.5 mg/L (Cd0.5), and 1 mg/L (Cd1), respectively. Note that *Pseudomonas*, *Sulfitobacter*, and *Sphingomonas* were highly antibiotic-resistant. *Flectobacillus* and *Fluviicola* were highly Pb-resistant. *Hydrogenophaga* was Hg-resistant, and both *Aestuariibacter* and *Pelomonas* were co-resistant to Pb and Cd. Abbreviations: Actinobacteria (Actino), Alphaproteobacteria (Alpha), Bacteroidetes (Bact), Betaproteobacteria (Beta), Gammaproteobacteria (Gamma), and Verrucomicrobia (Verruco).

this reasoning cannot explain the results for *P. bursaria*, in which the assemblage structure of DRB across multiple environmental gradients appeared to be less variable than that of environmental bacterioplankton. The contrasting variability of DRB in *P. bursaria* and *E. vannus* may be related to their nutritional models (mixotrophy vs. heterotrophy), in which the mixotrophs have a highly flexible physiology to cope with the changing environment by shifting between phototrophic and phagotrophic lifestyles. The characteristic intracellular environment of mixotrophs thus selects a narrow spectrum of bacterial species to reside intracellularly.

The selection of DRB in all the treatments investigated in this study may be related to the direct influence of environmental factors and pollution stresses on the physiology and biochemistry of the protists, which may affect the interactions between the predators and preys. At a higher temperature (not higher than the optimal temperature), a protist usually has a high growth rate (Montagnes and Weisse, 2000), ingestion rate (Izaguirre et al., 2012), and digestion rate (Sherr et al., 1988). Compared to the light condition, protozoan ingestion rate determined by using fluorescently labeled prey was lower under the dark conditions (Izaguirre et al., 2012). Light availability is important for mixotrophs. For example, *Chlorella* symbionts provide photosynthetic products to their host under light conditions (Shibata et al., 2016), but they lost their ability to resist host digestion in darkness (Kodama and Fujishima, 2014). Heavy metals also affect protistan ingestion rates (Al-Rasheid and Sleigh, 1994) and physiology (Kim et al., 2011).

The bacterial species associated with the protistan grazers may be related to not only the life stage and physiology of ciliates (Xu et al., 2020), but also depend on the biological nature (e.g., digestibility) of these bacteria (Zou et al., 2020), which are more or less reflected by their phylogenetic classification. Our analyses of clone libraries revealed that the overall DRB assemblage composition in *E. vannus* across all treatments was dominated by Gamma- and Alphaproteobacteria, which was consistent with previous reports for a range of marine ciliate species and picoeukaryotes (Farnelid et al., 2016; Gong et al., 2016). However, this compositional trait of DRB was not applicable for the DRB in the freshwater species *P. bursaria*, in which Gammaproteobacteria, Bacteroidetes, and Betaproteobacteria were the most abundant three taxa. The high proportions of Bacteroidetes and Betaproteobacteria could be due to their generally high abundance in freshwater systems (Newton et al., 2011). The phylum Bacteroidetes is well known for its high abundance in the gut microbiota (Mahowald et al., 2009) and for having a special protein secretion system (Type IX Secretion System, T9SS) that ensures cell survival and fitness in response to its habitat (Lasica et al., 2017). It is likely that habitat (freshwater-marine) distinctness in higher taxonomic composition of DRB exists, but it is a notion that needs to be further investigated for more freshwater protist species. At lower taxonomic ranks, the DRB assemblage composition and structure along different environmental gradients and pollutant stresses showed many interesting characteristics, many of which are reported for the first time in this study, and the underlying mechanisms are discussed below.

Warming Selected Specific Bacterial Species in Association With Protists

It is interesting to observe that *Pseudomonas* spp., as a dominant group in *P. bursaria*, had higher relative abundances at higher temperatures (**Figure 4A**). It was possible that the endosymbiotic green algae *Chlorella* sp. became more carbon-rich at higher temperatures (Serra-Maia et al., 2016), which could supply more organic matter to the symbiotic *Pseudomonas* species (Yao et al., 2019). An opposite trend was observed for the dominant DRB group in the algae-free ciliate *E. vannus*, in which the relative abundance of *Pseudoalteromonas* species decreased progressively with the increase of temperature (**Figure 4A**). The cellular chemical composition of *E. vannus* could be altered with temperature, with decreasing carbon to nitrogen ratio or phosphorus ratio at higher temperatures, according to the ecological stoichiometry theory (Woods et al., 2003; Fu and Gong, 2017). This temperature-driven stoichiometric shift in the host could select against specific heterotrophic DRB populations, such as *Pseudoalteromonas* spp. The lower relative abundance of *Pseudoalteromonas* occurred at a higher temperature (25°C), which could be attributed to the mechanism whereby *Pseudoalteromonas* kills other bacterial competitors, such as *Vibrio,* by secreting pseudoalterin, a thermolabile protease (Richards et al., 2017; Tang et al., 2020), which might lower the killing activity at a higher temperature, resulting in a higher proportion of co-occurring *Vibrio* in the DRB assemblage. Also, a higher temperature might enrich the type III secretion system (T3SS) of *Vibrio* in association with protists (Matz et al., 2011).

Light-Driven DRB Assemblage in the Heterotrophic Protist, but Light-Independent DRB in the Mixotroph

The DRB assemblage significantly responded to the light conditions, which occurred only in the heterotrophic *E. vannus* but not in the mixotrophic *P. bursaria*, indicating that the mixotroph could select specific bacterial populations. Interestingly, the DRB detected in the *P. bursaria*, i.e., the gammaproteobacterial *Nevskia* and the alphaproteobacterial *Caulobacter* and *Asticcacaulis*, share a common morphological character in having a stalk or holdfast at certain life stages, with which cells are able to attach onto a water-air interface or substrate surface (Stürmeyer et al., 1998; Purcell et al., 2007; Persat and Gitai, 2014). Typical species of the former two genera have also been demonstrated to be light-sensitive. For example, *Nevskia ramosa* often inhabit at the air-water interface and is capable of DNA reparation against UV damage (Stürmeyer et al., 1998). Visible light can act to regulate a sensory module in *Caulobacter crescentus* in order to increase the biochemical activity and cellular signaling for cell–surface and cell–cell attachment (Purcell et al., 2007). *Asticcacaulis* was detected in the microbial consortium of the oil-rich green alga *Botryococcus braunii* (Sambles et al., 2017). In the constant light treatment, continuous uptake of nutrients by the autotrophs, which included those in medium and the *Chlorella* symbionts inside the *P. bursaria*, probably lead to nutrient limitation to heterotrophic bacteria in the medium. Attachments to, or residue

of these bacteria inside the ciliate cell may facilitate themselves to immediately "capture" the nutrients regenerated by the protist. In constant darkness, *P. bursaria* might sustain by bacterivory, and the bacteria-protist association might reduce bacterial mortality. Therefore, our study based on light manipulation and single cell analysis of protists provides evidence that mixotrophic protists are previously unrecognized hosts and micro-niches of these attaching bacteria in natural environments.

The *Curvibacter* phylotype occurred as DRB of the *P. bursaria* in all-light, all-dark, and diel-cycle treatments. Cultivation in constant darkness or at night might lower the concentration of dissolved oxygen, which provides an ecological advantage to microaerobic bacteria, such as *Curvibacter* sp. (Ding and Yokota, 2010). It has been demonstrated that members of this genus are able to inhibit fungal infection by interacting with other commensal bacterial species in the cnidarian *Hydra* (Fraune et al., 2015). In fact, at least filament fungi were recognizable via the naked eye at later periods of the cultures supplied with rice grains, indicating a risk of fungal infection of the *P. bursaria*. In this sense, it is possible for these bacterial consortiums to function in anti-fungal activity. The *Variovorax* phylotypes were only detected in both LL and LD treatments of the *P. bursaria*. This adaptive ability in such contrasting light environments is consistent with a previous study, which showed a combination of autotrophic and heterotrophic features in the genome of *Variovorax paradoxus* (Han et al., 2011).

The DRB in the heterotrophic ciliate *E. vannus* were photoperiod-dependent. *Alteromonas* sp. was dominant in the treatment of the diel light:dark cycles, suggesting a role of light (or darkness) in selecting these bacteria in association with the protistan cell. A similar mechanism was proposed by a previous study (Biller et al., 2018), which stated that *Alteromonas* may provide energy or organic compounds to cyanobacteria *Prochlorococcus* under the stress of darkness. The *Pseudoalteromonas* phylotypes were consistently present in the DRB assemblages under the conditions having a photic period, probably contributing to anti-fungal infection by more actively producing antifungal polyketide alteramides during the dark period (Moree et al., 2014). Thus, the co-occurrence of these two bacterial taxa may be of benefit to the host for a balance between rapid growth and low pathogenic infection under a natural diel light-dark condition (Liu et al., 2019).

Evidence for Prevalent Antibiotic-Resistant Bacteria Sheltered in Protistan Cells

Gomiero and Viarengo (2014) showed that the antibiotic OTC (3.2 μM to 32 mM) treatments induced changes in the growth, survival, endocytosis rate, and lysosomal membrane stability of the marine ciliate *Euplotes crassus*. Such physiological shifts might have also occurred in these two species we investigated. Apart from that, we found the dominant DRB in the OTC-treated marine ciliate *E. vannus* were affiliated with the members of the genus *Sphingomonas* and the family *Alteromonadaceae* (*Alteromonas* and *Aestuariibacter*) (**Figure 5A**), which is in line with previous findings that both *Sphingomonas* and *Alteromonas*

species were resistant to antibiotics, such as OTC (Miranda and Zemelman, 2002; Dang et al., 2007). However, the relative abundance of the phylotype of the family *Puniceicoccaceae* (phylum Verrucomicrobia) decreased in OTC10 and was non-detectable in OTC20, indicating it is sensitive to OTC.

Both *Pseudomonas* and *Sulfitobacter* phylotypes prevailed in the DRB assemblage of mixotrophic *P. bursaria* reared in media with an antibiotic concentration up to 20 mg/L, indicating high antibiotic resistance of these bacteria and that the intracellular environment may provide a favorable habitat for their survival. Indeed, it has been demonstrated that many *Pseudomonas* species could degrade antibiotics via efflux pumps (e.g., Jiang et al., 2014), and consortiums of these bacterial species with algae could enhance the efficiency of degrading antibiotics (Leng et al., 2020). Similarly, genes involved in aromatic compound catabolism and a type IV secretion system are present in the genome of a strain of *Sulfitobacter* (Ankrah et al., 2014), and *Sulfitobacter* in the diatom phycosphere could supply indole acetic acid to the algae in exchange for organosulfur compounds (Amin et al., 2015). Furthermore, *Sulfitobacter* strains isolated from marine hydrothermal vent fields were found to be antibiotic-resistant (Farias et al., 2015). All these suggest that the mixotrophic protist bearing endosymbiotic microalgae (e.g., *Chlorella* sp.) could play a role in accommodating these antibiotic-resistant bacteria, which represent a previously unrecognized scenario in the antibiotic resistance of environmental bacterial populations.

Bacterial Co-resistance to Heavy Metals and to Protistan Digestions

It is well known that short-rod cells of *Flectobacillus* form long filaments and chains of several cells, a morphology-based strategy to protect themselves from being ingested by nanoflagellates predators (Corno and Jürgens, 2006). We detected these bacteria as a member of DRB in *P. bursaria*, suggesting an effect of predator size in the prey-predator interactions, i.e., enlarged bacterial cell size may be effective to avoid being engulfed by small protists but not necessarily for large-celled protists, such as ciliates with wide or highly contractile cytostomes. Furthermore, the *Flectobacillus* phylotypes became dominant in the Pb-treated cultures, demonstrating they are co-resistant to Pb and protistan digestion. However, *Flectobacillus* spp. were found to be a dominant bacterial group in the riverbed sediments spiked with high concentrations of metals, including Cd and Cu, but not in the Pb and Cr treatments (Du et al., 2018). In the Hg-treated *P. bursaria* culture, we also found that *Flectobacillus* phylotypes only accounted for a minor portion of DRB. This suggests a strain-level differentiation in the heavy metal resistance of *Flectobacillus*.

Acinetobacter junii is able to form biofilms on surfaces to resistant to mercury (Sarkar and Chakraborty, 2008), which is in line with our observation of its survival in *P. bursaria* under Hg stresses. In addition, our results point to the non-digestible nature of this bacterial species in ciliated protozoa, highlighting its ecological success in natural environments. Furthermore, *Hydrogenophaga* was also abundant in *P. bursaria* treated with a

high dose of Hg. It remains to be investigated how this hydrogen-oxidizing species interacts with the host and endosymbiotic green alga within the *P. bursaria* under Hg stress, though it is known that As (III) could be oxidized by a strain of this genus under aerobic conditions (Terry et al., 2015).

Not much is known about the ecology and microbial association of *Aestuariibacter*, except for our recent report of this genus as a DRB in four marine and one freshwater species of ciliates (Gong et al., 2016). In the present study, we once again found this genus as a dominant group of DRB in *E. vannus* across all Pb^{2+} and Cd^{2+} treatments and under low-dose antibiotic treatment, indicating *Aestuariibacter* is a previously unrecognized superstar in co-resistance to heavy metals, antibiotics, and protistan digestion. This is probably due to their resident habitats of high-pollution stresses, such as coastal seawater and tidal flats (Yi et al., 2004; Wang et al., 2010). *Pelomonas* was present in the DRB of *E. vannus* treated with high doses of Pb^{2+} and Cd^{2+} but absent in the controls, indicating the metal tolerance of this group. Phylotypes of this genus were also detected in Cd- and Cu-treated activated sludge using DGGE and sequencing (Bhat et al., 2020). Strains of Verrucomicrobia have been isolated as gut symbionts from sea cucumber, marine sponges, clamworm (Wertz et al., 2012), and the marine ciliate *Euplotidium* (Petroni et al., 2000). Our study showed the association between a possible new genus of the family *Puniceicoccaceae* with the ciliate *E. vannus* and for the first time their differential resistance to metals Pb and Cd.

CONCLUDING REMARKS

As major players in the microbial loop and biogeochemical cycle within ecosystems, both bacteria and protists are ecologically linked not only through prey-predator food chains but also via collaboration in facing multiple stresses. Our study reveals for the first time that the assemblage composition and structure of ingested but inedible bacteria in two protists vary significantly in response to stresses of temperature, light, antibiotics, and heavy metals, indicating that the environment plays an important role in selecting specific bacterial populations in protist-bacteria associations. Our results for these two ciliate species also provide an indication that trophic mode of protists (mixotrophs vs. heterotrophs) could be a factor influencing the bacteria-protist interactions, a notion warrants further investigation considering their increasingly recognized importance in marine food webs (Stoecker et al., 2017). Furthermore, bacterial antibiotic resistance and metal resistance have been extensively studied in the past several decades. The ecological interactions between these resistant bacteria and protists remain poorly understudied (Nguyen et al., 2020). Our findings in this study provide evidence that there are diverse bacterial stains, which are not only resistant to antibiotics and/or heavy metals in natural environments but have also survived protistan digestion, suggesting some bacterial species/strains could use protistan cells as shelters in facing of pollution stresses.

DATA AVAILABILITY STATEMENT

The datasets presented in this study can be found in online repositories. The names of the repositories and accession numbers can be found in the article/**Supplementary Material**.

AUTHOR CONTRIBUTIONS

SZ did the data curation-equal, formal analysis-equal, investigation-equal, methodology-equal, resources-equal, software-equal, validation-equal, visualization-equal, and wrote the original draft-lead. QZ performed the resources-supporting and validation-supporting. XZ and CD performed the validation-supporting. JG performed the conceptualization-lead, data curation-supporting, funding acquisition-lead, methodology-equal, project administration-lead, resources-equal, supervision-equal, validation-equal, and wrote, reviewed and edited the manuscript-lead. All authors contributed to the article and approved the submitted version.

FUNDING

SUPPLEMENTARY MATERIAL

The Supplementary Material for this article can be found online at: https://www.frontiersin.org/articles/10.3389/fmars.2020.00659/full#supplementary-material

FIGURE S1 | A general scheme of research methodology.

REFERENCES

Adams, H. E., Crump, B. C., and Kling, G. W. (2010). Temperature controls on aquatic bacterial production and community dynamics in arctic lakes and streams. *Environ. Microbiol.* 12, 1319–1333. doi: 10.1111/j.1462-2920.2010.02176.x

Alonso-Sáez, L., Gasol, J. M., Lefort, T., Hofer, J., and Sommaruga, R. (2006). Effect of natural sunlight on bacterial activity and differential sensitivity of natural bacterioplankton groups in northwestern mediterranean coastal waters. *Appl. Environ. Microbiol.* 72, 5806–5813. doi: 10.1128/AEM.00597-06

Al-Rasheid, K. A. S., and Sleigh, M. A. (1994). The effects of heavy metals on the feeding rate of *Euplotes mutabilis* (Tuffrau, 1960). *Eur. J. Protistol.* 30, 270–279. doi: 10.1016/S0932-4739(11)80073-8

Amin, S. A., Hmelo, L. R., Van Tol, H. M., Durham, B. P., Carlson, L. T., Heal, K. R., et al. (2015). Interaction and signalling between a cosmopolitan phytoplankton and associated bacteria. *Nature* 522, 98–101. doi: 10.1038/nature14488

Ankrah, N. Y. D., Lane, T., Budinoff, C. R., Hadden, M. K., and Buchan, A. (2014). Draft genome sequence of *Sulfitobacter* sp. CB2047, a member of the *Roseobacter clade* of marine bacteria, isolated from an *Emiliania huxleyi* bloom. *Genome Announc.* 2:e001125-14. doi: 10.1128/genomeA.01125-14

Asheford, K. E., Chuzhanova, N. A., Fry, J. C., Jones, A. J., and Weightman, A. J. (2006). New screening software shows that most recent large 16S rRNA gene clone libraries contain chimeras. *Appl. Environ. Microbiol.* 72, 5734–5741. doi: 10.1128/AEM.00556-06

Azam, F., Fenchel, T., Field, J. G., Gray, J. S., Meyer-Reil, L. A., and Thingstad, F. (1983). The ecological role of water-column microbes in the sea. *Mar. Ecol. Prog. Ser.* 10, 257–263. doi: 10.3354/meps010257

Bhat, S. A., Cui, G., Li, W., Wei, Y., and Li, F. (2020). Effect of heavy metals on the performance and bacterial profiles of activated sludge in a semi-continuous reactor. *Chemosphere* 241:125035. doi: 10.1016/j.chemosphere.2019.125035

Biller, S. J., Coe, A., Roggensack, S. E., and Chisholm, S. W. (2018). Heterotroph interactions alter *Prochlorococcus* transcriptome dynamics during extended periods of darkness. *mSystems* 3:e0040-18. doi: 10.1128/mSystems.00040-18

Boenigk, J., Matz, C., Jürgens, K., and Arndt, H. (2001). The influence of preculture conditions and food quality on the ingestion and digestion process of three species of heterotrophic nanoflagellates. *Microb. Ecol.* 42, 168–176. doi: 10.1007/s002480000116

Corno, G., and Jürgens, K. (2006). Direct and indirect effects of protist predation on population size structure of a bacterial strain with high phenotypic plasticity. *Appl. Environ. Microbiol.* 72, 78–86. doi: 10.1128/AEM.72.1.78-86.2006

Dang, H., Zhang, X., Song, L., Chang, Y., and Yang, G. (2007). Molecular determination of oxytetracycline-resistant bacteria and their resistance genes from mariculture environments of China. *J. Appl. Microbiol.* 103, 2580–2592. doi: 10.1111/j.1365-2672.2007.03494.x

Darriba, D., Taboada, G. L., Doallo, R., and Posada, D. (2012). jModelTest 2: more models, new heuristics and parallel computing. *Nat. Methods* 9, 772–772. doi: 10.1038/nmeth.2109

Ding, L., and Yokota, A. (2010). *Curvibacter fontana* sp. nov., a microaerobic bacteria isolated from well water. *J. Gen. Appl. Microbiol.* 56, 267–271. doi: 10.2323/jgam.56.267

Du, H., Harata, N., and Li, F. (2018). Responses of riverbed sediment bacteria to heavy metals: integrated evaluation based on bacterial density, activity and community structure under well-controlled sequencing batch incubation conditions. *Water Res.* 130, 115–126. doi: 10.1016/j.watres.2017.10.070

Farias, P., Espírito Santo, C., Branco, R., Francisco, R., Santos, S., Hansen, L., et al. (2015). Natural hot spots for gain of multiple resistances: arsenic and antibiotic resistances in heterotrophic, aerobic bacteria from marine hydrothermal vent fields. *Appl. Environ. Microbiol.* 81, 2534–2543. doi: 10.1128/AEM.03240-14

Farnelid, H. M., Turk-Kubo, K. A., and Zehr, J. P. (2016). Identification of associations between bacterioplankton and photosynthetic picoeukaryotes in coastal waters. *Front. Microbiol.* 7:339. doi: 10.3389/fmicb.2016.00339

First, M. R., Park, N. Y., Berrang, M. E., Meinersmann, R. J., Bernhard, J. M., Gast, R. J., et al. (2012). Ciliate ingestion and digestion: flow cytometric measurements and regrowth of a digestion-resistant *Campylobacter jejuni*. *J. Eukaryot. Microbiol.* 59, 12–19. doi: 10.1111/j.1550-7408.2011.00589.x

Fraune, S., Anton-Erxleben, F., Augustin, R., Franzenburg, S., Knop, M., Schröder, K., et al. (2015). Bacteria-bacteria interactions within the microbiota of the ancestral metazoan *Hydra* contribute to fungal resistance. *ISME J.* 9, 1543–1556. doi: 10.1038/ismej.2014.239

Fu, R., and Gong, J. (2017). Single cell analysis linking ribosomal (r)DNA and rRNA copy numbers to cell size and growth rate provides insights into molecular protistan ecology. *J. Eukaryot. Microbiol.* 64, 885–896. doi: 10.1111/jeu.12425

Galtier, N., Gouy, M., and Gautier, C. (1996). SEAVIEW and PHYLO_WIN: two graphic tools for sequence alignment and molecular phylogeny. *Bioinformatics* 12, 543–548. doi: 10.1093/bioinformatics/12.6.543

Gomiero, A., and Viarengo, A. (2014). Effects of elevated temperature on the toxicity of copper and oxytetracycline in the marine model, *Euplotes crassus*: a climate change perspective. *Environ. Pollut.* 194, 262–271. doi: 10.1016/j.envpol.2014.07.035

Gong, J., Qing, Y., Guo, X., and Warren, A. (2014). "*Candidatus Sonnebornia yantaiensis*", a member of candidate division OD1, as intracellular bacteria of the ciliated protist *Paramecium bursaria* (Ciliophora. Oligohymenophorea). *Syst. Appl. Microbiol.* 37, 35–41. doi: 10.1016/j.syapm.2013.08.007

Gong, J., Qing, Y., Zou, S., Fu, R., Su, L., Zhang, X., et al. (2016). Protist-bacteria associations: gammaproteobacteria and alphaproteobacteria are prevalent as digestion-resistant bacteria in ciliated protozoa. *Front. Microbiol.* 7:498. doi: 10.3389/fmicb.2016.00498

Guindon, S., Delsuc, F., Dufayard, J.-F., and Gascuel, O. (2009). "Estimating maximum likelihood phylogenies with PhyML," in *Bioinformatics for DNA Sequence Analysis. Methods in Molecular Biology*, ed. D. Posada (Totowa, NJ: Humana Press), 113–137. doi: 10.1007/978-1-59745-251-9_6

Han, J.-I., Choi, H.-K., Lee, S.-W., Orwin, P. M., Kim, J., Laroe, S. L., et al. (2011). Complete genome sequence of the metabolically versatile plant growth-promoting endophyte *Variovorax paradoxus* S110. *J. Bacteriol.* 193, 1183–1190. doi: 10.1128/JB.00925-10

Hu, A., Yang, X., Chen, N., Hou, L., Ma, Y., and Yu, C.-P. (2014). Response of bacterial communities to environmental changes in a mesoscale subtropical watershed, Southeast China. *Sci. Total Environ.* 472, 746–756. doi: 10.1016/j.scitotenv.2013.11.097

Huber, T., Faulkner, G., and Hugenholtz, P. (2004). Bellerophon: a program to detect chimeric sequences in multiple sequence alignments. *Bioinformatics* 20, 2317–2319. doi: 10.1093/bioinformatics/bth226

Ibekwe, A. M., Ma, J., and Murinda, S. E. (2016). Bacterial community composition and structure in an urban river impacted by different pollutant sources. *Sci. Total Environ.* 566–567, 1176–1185. doi: 10.1016/j.scitotenv.2016.05.168

Izaguirre, I., Sinistro, R., Schiaffino, M. R., Sánchez, M. L., Unrein, F., and Massana, R. (2012). Grazing rates of protists in wetlands under contrasting light conditions due to floating plants. *Aquat. Microb. Ecol.* 65, 221–232. doi: 10.3354/ame01547

Jiang, B., Li, A., Cui, D., Cai, R., Ma, F., and Wang, Y. (2014). Biodegradation and metabolic pathway of sulfamethoxazole by *Pseudomonas psychrophila* HA-4, a newly isolated cold-adapted sulfamethoxazole-degrading bacterium. *Appl. Microbiol. Biotechnol.* 98, 4671–4681. doi: 10.1007/s00253-013-5488-3

Jousset, A. (2012). Ecological and evolutive implications of bacterial defences against predators. *Environ. Microbiol.* 14, 1830–1843. doi: 10.1111/j.1462-2920.2011.02627.x

Katoh, K., and Standley, D. M. (2013). MAFFT multiple sequence alignment software version 7: improvements in performance and usability. *Mol. Biol. Evol.* 30, 772–780. doi: 10.1093/molbev/mst010

Kim, S.-H., Jung, M.-Y., and Lee, Y.-M. (2011). Effect of heavy metals on the antioxidant enzymes in the marine ciliate *Euplotes crassus*. *Toxicol. Environ. Health Sci.* 3, 213–219. doi: 10.1007/s13530-011-0103-4

Kodama, Y., and Fujishima, M. (2014). Symbiotic *Chlorella variabilis* incubated under constant dark conditions for 24 hours loses the ability to avoid digestion by host lysosomal enzymes in digestive vacuoles of host ciliate *Paramecium bursaria*. *FEMS Microbiol. Ecol.* 90, 946–955. doi: 10.1111/1574-6941.12448

Lane, D. J. (1991). *16S/23S rRNA Sequencing*. New York, NY: John Wiley & Sons Ltd.

Lasica, A. M., Ksiazek, M., Madej, M., and Potempa, J. (2017). The type IX secretion system (T9SS): highlights and recent insights into its structure and function. *Front. Cell. Infect. Microbiol.* 7:215. doi: 10.3389/fcimb.2017.00215

Leng, L., Wei, L., Xiong, Q., Xu, S., Li, W., Lv, S., et al. (2020). Use of microalgae based technology for the removal of antibiotics from wastewater: a review. *Chemosphere* 238:124680. doi: 10.1016/j.chemosphere.2019.124680

Liu, J., Meng, Z., Liu, X., and Zhang, X.-H. (2019). Microbial assembly, interaction, functioning, activity and diversification: a review derived from community compositional data. *Mar. Life Sci. Technol.* 1, 112–128. doi: 10.1007/s42995-019-00004-3

Mahowald, M. A., Rey, F. E., Seedorf, H., Turnbaugh, P. J., Fulton, R. S., Wollam, A., et al. (2009). Characterizing a model human gut microbiota composed of members of its two dominant bacterial phyla. *Proc. Natl. Acad. Sci. U.S.A.* 106, 5859–5864. doi: 10.1073/pnas.0901529106

Martinez-Garcia, M., Brazel, D., Poulton, N. J., Swan, B. K., Gomez, M. L., Masland, D., et al. (2012). Unveiling in situ interactions between marine protists and bacteria through single cell sequencing. *ISME J.* 6, 703–707. doi: 10.1038/ismej.2011.126

Matz, C., and Kjelleberg, S. (2005). Off the hook-how bacteria survive protozoan grazing. *Trends Microbiol.* 13, 302–307. doi: 10.1016/j.tim.2005.05.009

Matz, C., Nouri, B., Mccarter, L., and Martinez-Urtaza, J. (2011). Acquired type III secretion system determines environmental fitness of epidemic *Vibrio*

parahaemolyticus in the interaction with bacterivorous protists. *PLoS One* 6:e20275. doi: 10.1371/journal.pone.0020275

Miranda, C. D., and Zemelman, R. (2002). Bacterial resistance to oxytetracycline in Chilean salmon farming. *Aquaculture* 212, 31–47. doi: 10.1016/S0044-8486(02) 00124-2

Montagnes, D. J. S., and Weisse, T. (2000). Fluctuating temperatures affect growth and production rates of planktonic ciliates. *Aquat. Microb. Ecol.* 21, 97–102. doi: 10.3354/ame021097

Moree, W. J., Mcconnell, O. J., Nguyen, D. D., Sanchez, L. M., Yang, Y.-L., Zhao, X., et al. (2014). Microbiota of healthy corals are active against fungi in a light-dependent manner. *ACS Chem. Biol.* 9, 2300–2308. doi: 10.1021/cb500432j

Newton, R. J., Jones, S. E., Eiler, A., Mcmahon, K. D., and Bertilsson, S. (2011). A guide to the natural history of freshwater lake bacteria. *Microbiol. Mol. Biol. Rev.* 75, 14–49. doi: 10.1128/MMBR.00028-10

Nguyen, B.-A. T., Chen, Q.-L., He, J.-Z., and Hu, H.-W. (2020). Microbial regulation of natural antibiotic resistance: understanding the protist-bacteria interactions for evolution of soil resistome. *Sci. Total Environ.* 705:135882. doi: 10.1016/j.scitotenv.2019.135882

Osborn, A. M., Moore, E. R. B., and Timmis, K. N. (2000). An evaluation of terminal-restriction fragment length polymorphism (T-RFLP) analysis for the study of microbial community structure and dynamics. *Environ. Microbiol.* 2, 39–50. doi: 10.1046/j.1462-2920.2000.00081.x

Pernthaler, J. (2005). Predation on prokaryotes in the water column and its ecological implications. *Nat. Rev. Microbiol.* 3, 537–546. doi: 10.1038/nrmicro1180

Persat, A., and Gitai, Z. (2014). Bacterial evolution: rewiring modules to get in shape. *Curr. Biol.* 24, R522–R524. doi: 10.1016/j.cub.2014.04.022

Petroni, G., Spring, S., Schleifer, K.-H., Verni, F., and Rosati, G. (2000). Defensive extrusive ectosymbionts of *Euplotidium* (Ciliophora) that contain microtubule-like structures are bacteria related to Verrucomicrobia. *Proc. Natl. Acad. Sci. U.S.A.* 97, 1813–1817. doi: 10.1073/pnas.030438197

Pucciarelli, S., Devaraj, R. R., Mancini, A., Ballarini, P., Castelli, M., Schrallhammer, M., et al. (2015). Microbial consortium associated with the antarctic marine ciliate *Euplotes focardii*: an investigation from genomic sequences. *Microb. Ecol.* 70, 484–497. doi: 10.1007/s00248-015-0568-9

Purcell, E. B., Siegal-Gaskins, D., Rawling, D. C., Fiebig, A., and Crosson, S. (2007). A photosensory two-component system regulates bacterial cell attachment. *Proc. Natl. Acad. Sci. U.S.A.* 104, 18241–18246. doi: 10.1073/pnas.0705887104

Richards, G. P., Watson, M. A., Needleman, D. S., Uknalis, J., Boyd, E. F., and Fay, J. P. (2017). Mechanisms for *Pseudoalteromonas piscicida*-induced killing of *vibrios* and other bacterial pathogens. *Appl. Environ. Microbiol.* 83:e00175-17. doi: 10.1128/AEM.00175-17

Ronquist, F., and Huelsenbeck, J. P. (2003). MrBayes 3: Bayesian phylogenetic inference under mixed models. *Bioinformatics* 19, 1572–1574. doi: 10.1093/bioinformatics/btg180

Sambles, C., Moore, K., Lux, T. M., Jones, K., Littlejohn, G. R., Gouveia, J. D., et al. (2017). Metagenomic analysis of the complex microbial consortium associated with cultures of the oil-rich alga *Botryococcus braunii*. *MicrobiologyOpen* 6:e00482. doi: 10.1002/mbo3.482

Sarkar, S., and Chakraborty, R. (2008). Quorum sensing in metal tolerance of *Acinetobacter junii* BB1A is associated with biofilm production. *FEMS Microbiol. Lett.* 282, 160–165. doi: 10.1111/j.1574-6968.2008.01080.x

Schloss, P. D., Westcott, S. L., Ryabin, T., Hall, J. R., Hartmann, M., Hollister, E. B., et al. (2009). Introducing mothur: open-source, platform-independent, community-supported software for describing and comparing microbial communities. *Appl. Environ. Microbiol.* 75, 7537–7541. doi: 10.1128/AEM.01541-09

Serra-Maia, R., Bernard, O., Gonçalves, A., Bensalem, S., and Lopes, F. (2016). Influence of temperature on *Chlorella vulgaris* growth and mortality rates in a photobioreactor. *Algal Res.* 18, 352–359. doi: 10.1016/j.algal.2016.06.016

Sherr, B. F., Sherr, E. B., and Rassoulzadegan, F. (1988). Rates of digestion of bacteria by marine phagotrophic protozoa: temperature dependence. *Appl. Environ. Microbiol.* 54, 1091–1095. doi: 10.1128/aem.54.5.1091-1095.1988

Shibata, A., Takahashi, F., Kasahara, M., and Imamura, N. (2016). Induction of maltose release by light in the endosymbiont *Chlorella variabilis* of *Paramecium bursaria*. *Protist* 167, 468–478. doi: 10.1016/j.protis.2016.08.007

Šimek, K., Kasalický, V., Jezbera, J., Horňák, K., Nedoma, J., Hahn, M. W., et al. (2013). Differential freshwater flagellate community response to bacterial food quality with a focus on *Limnohabitans* bacteria. *ISME J.* 7, 1519–1530. doi: 10.1038/ismej.2013.57

Stoecker, D. K., Hansen, P. J., Caron, D. A., and Mitra, A. (2017). Mixotrophy in the marine plankton. *Ann. Rev. Mar. Sci.* 9, 311–335. doi: 10.1146/annurev-marine-010816-060617

Storesund, J. E., Erga, S. R., Ray, J. L., Thingstad, T. F., and Sandaa, R.-A. (2015). Top-down and bottom-up control on bacterial diversity in a western Norwegian deep-silled fjord. *FEMS Microbiol. Ecol.* 91:fiv076. doi: 10.1093/femsec/fiv076

Stürmeyer, H., Overmann, J., Babenzien, H.-D., and Cypionka, H. (1998). Ecophysiological and phylogenetic studies of *Nevskia ramosa* in pure culture. *Appl. Environ. Microbiol.* 64, 1890–1894. doi: 10.1128/aem.64.5.1890-1894.1998

Tang, B.-L., Yang, J., Chen, X.-L., Wang, P., Zhao, H.-L., Su, H.-N., et al. (2020). A predator-prey interaction between a marine *Pseudoalteromonas* sp. and *Gram-positive* bacteria. *Nat. Commun.* 11:285. doi: 10.1038/s41467-019-14133-x

Terry, L. R., Kulp, T. R., Wiatrowski, H., Miller, L. G., and Oremland, R. S. (2015). Microbiological oxidation of antimony (III) with oxygen or nitrate by bacteria isolated from contaminated mine sediments. *Appl. Environ. Microbiol.* 81, 8478–8488. doi: 10.1128/AEM.01970-15

Wang, Q., Garrity, G. M., Tiedje, J. M., and Cole, J. R. (2007). Naïve bayesian classifier for rapid assignment of rRNA sequences into the new bacterial taxonomy. *Appl. Environ. Microbiol.* 73, 5261–5267. doi: 10.1128/AEM.00062-07

Wang, Y., Wang, H., Liu, J., Lai, Q., Shao, Z., Austin, B., et al. (2010). *Aestuariibacter aggregatus* sp. nov., a moderately *Halophilic* bacterium isolated from seawater of the Yellow Sea. *FEMS Microbiol. Lett.* 309, 48–54. doi: 10.1111/j.1574-6968.2010.02011.x

Wertz, J. T., Kim, E., Breznak, J. A., Schmidt, T. M., and Rodrigues, J. L. M. (2012). Genomic and physiological characterization of the Verrucomicrobia isolate *Diplosphaera colitermitum* gen. nov., sp. nov., reveals microaerophily and nitrogen fixation genes. *Appl. Environ. Microbiol.* 78, 1544–1555. doi: 10.1128/AEM.06466-11

Woods, H. A., Makino, W., Cotner, J. B., Hobbie, S. E., Harrison, J. F., Acharya, K., et al. (2003). Temperature and the chemical composition of poikilothermic organisms. *Funct. Ecol.* 17, 237–245. doi: 10.1046/j.1365-2435.2003.00724.x

Xu, Y., Shen, Z., Gentekaki, E., Xu, J., and Yi, Z. (2020). Comparative transcriptome analyses during the vegetative cell cycle in the mono-cellular organism *Pseudokeronopsis erythrina* (Alveolata, Ciliophora). *Microorganisms* 8:108. doi: 10.3390/microorganisms8010108

Yao, S., Lyu, S., An, Y., Lu, J., Gjermansen, C., and Schramm, A. (2019). Microalgae-bacteria symbiosis in microalgal growth and biofuel production: a review. *J. Appl. Microbiol.* 126, 359–368. doi: 10.1111/jam.14095

Yi, H., Bae, K. S., and Chun, J. (2004). *Aestuariibacter salexigens* gen. nov., sp. nov. and *Aestuariibacter halophilus* sp. nov., isolated from tidal flat sediment, and emended description of *Alteromonas macleodii*. *Int. J. Syst. Evol. Microbiol.* 54, 571–576. doi: 10.1099/ijs.0.02798-0

Zou, S., Zhang, Q., and Gong, J. (2020). Comparative transcriptomics reveals distinct gene expressions of a model ciliated protozoan feeding on bacteria-free medium, digestible, and digestion-resistant bacteria. *Microorganisms* 8:559. doi: 10.3390/microorganisms8040559